AD-A102 206 ROCKWELL INTERNATIONAL THOUSAND OAKS CA SCIENCE CENTER F/G 11/6
SUPERPLASTIC FORMING & DIFFUSION BONDING OF CORONA 5.(U)
JUN 81 J C CHESNUTT, C H HAMILTON, C F YOLTON N00019-79-C-0465
UNCLASSIFIED SC5234.6FR NL

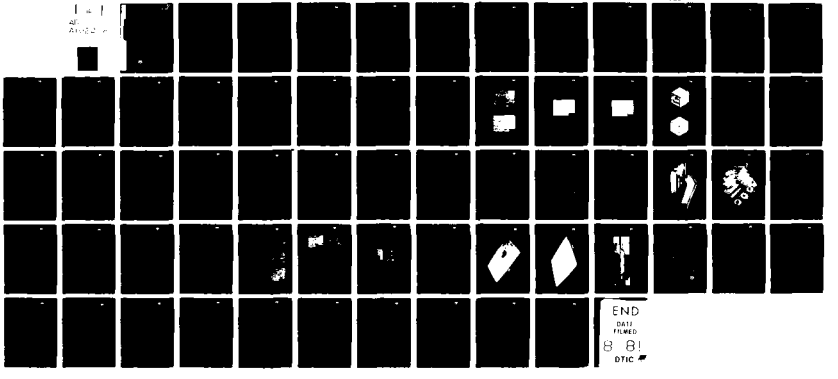

END
DATE FILMED
8 81
DTIC

SC5234.6FR

Copy No. 28

SUPERPLASTIC FORMING & DIFFUSION BONDING OF CORONA 5.

FINAL TECHNICAL REPORT FOR THE PERIOD
September 1, 1979 through November 30, 1980

CONTRACT NO. N00019-79-C-0465

Prepared for

Department of the Navy
Naval Air Systems Command
Washington, DC 20361

J.C. Chesnutt, C.H. Hamilton
C.F. Yolton

JUNE 1981

Approved for public release; distribution unlimited

Rockwell International
Science Center

UNCLASSIFIED

SECURITY CLASSIFICATION OF THIS PAGE (When Data Entered)

REPORT DOCUMENTATION PAGE	READ INSTRUCTIONS BEFORE COMPLETING FORM
1. REPORT NUMBER	2. GOVT ACCESSION NO. AD-A102 206	3. RECIPIENT'S CATALOG NUMBER
4. TITLE (and Subtitle) Superplastic Forming & Diffusion Bonding of CORONA 5	5. TYPE OF REPORT & PERIOD COVERED Final Technical Report 09/01/79 through 11/15/80
	6. PERFORMING ORG. REPORT NUMBER SC5234.6FR
7. AUTHOR(s) J.C. Chesnutt, C.H. Hamilton and C.F. Yolton	8. CONTRACT OR GRANT NUMBER(s) N00019-79-C-0465
9. PERFORMING ORGANIZATION NAME AND ADDRESS Rockwell International, Science Center 1049 Camino Dos Rios, Thousand Oaks, CA 91360	10. PROGRAM ELEMENT, PROJECT, TASK AREA & WORK UNIT NUMBERS
11. CONTROLLING OFFICE NAME AND ADDRESS Department of the Navy Naval Air Systems Command, Washington, DC 20361	12. REPORT DATE June, 1981
	13. NUMBER OF PAGES 62
14. MONITORING AGENCY NAME & ADDRESS(if different from Controlling Office)	15. SECURITY CLASS. (of this report) Unclassified
	15a. DECLASSIFICATION/DOWNGRADING SCHEDULE

16. DISTRIBUTION STATEMENT (of this Report)

Approved for public release; distribution unlimited

17. DISTRIBUTION STATEMENT (of the abstract entered in Block 20, if different from Report)

18. SUPPLEMENTARY NOTES

19. KEY WORDS (Continue on reverse side if necessary and identify by block number)

Superplastic forming, diffusion bonding, sheet-coil processing, titanium alloys, hot-rolling, cold-rolling, heat treatment, tensile properties.

20. ABSTRACT (Continue on reverse side if necessary and identify by block number)

The processing of CORONA 5 (Ti-4.5 Al-5 Mo-1.5 Cr) to cold-rolled sheet and the subsequent evaluation of this sheet for superplastic formability, diffusion bondability and post-forming heat treatment response is discussed. Two heats of CORONA 5, one of "standard" oxygen content (0.183 wt %) and one of low oxygen content (0.085 wt %) were processed to fine-grained, 0.07 in (1.8 mm) sheet and limited characterization of the sheet material conducted.

(continued)

DD FORM 1 JAN 73 1473 EDITION OF 1 NOV 65 IS OBSOLETE

UNCLASSIFIED

SECURITY CLASSIFICATION OF THIS PAGE (When Data Entered)

Superplastic properties were determined at 843, 871 and 899°C; diffusion bonding parameters were predicted for all three temperatures and evaluated at 871°C. Adequate superplastic properties were observed at all temperatures with the lower temperatures exhibiting better properties. The optimum superplastic forming and diffusion bonding temperature was found to be 871°C, particularly for low oxygen material. Pan forming tests at all three temperatures and the expanded sandwich test at 871°C confirmed these observations.

The low oxygen material was heat treatable after forming but the strengths achievable for air cool only were limited to approximately 862 MPa (125 ksi) yield strength and 965 MPa (140 ksi) ultimate tensile strength. The standard oxygen material in contrast responded more strongly to heat treatment with yield and tensile strengths of 1033 MPa (150 ksi) and 1134 MPa (165 ksi) possible, demonstrating a significant improvement over Ti-6Al-4V which would require a part distorting, water-quench to reach similar strength levels.

The results of the program have demonstrated that by controlling the oxygen content of CORONA 5 and by processing to a small grain size, a highly desirable combination of SPF/DB response and post-forming tensile properties could be obtained and that the alloy is amenable to sheet processing using a continuous-strip process.

TABLE OF CONTENTS

		Page
1.0	INTRODUCTION	1
2.0	EXPERIMENTAL PROCEDURES	3
2.1	Material Processing	3
2.1.1	Hot Rolling	3
2.1.2	Cold Rolling	4
2.2	Tensile Tests	5
2.3	Forming Tests	6
2.4	Diffusion Bonding Tests	7
2.5	SPF/DB Demonstration	8
2.6	Post Forming Heat Treatment	10
3.0	RESULTS AND DISCUSSION	12
3.1	Material Characterization	12
3.2	Tensile Tests	17
3.3	Forming Tests	27
3.4	Diffusion Bonding Tests	29
3.5	SPF/DB Sandwich	40
3.6	Post Forming Tensile Tests	46
4.0	CONCLUSIONS	49
5.0	ACKNOWLEDGMENTS	50
6.0	REFERENCES	51

LIST OF FIGURES

Figure		Page
1	Microstructure of as hot-rolled CORONA 5 hot band. (500X).....	13
2	Microstructure of standard oxygen CORONA 5 hot band after a simulated strand-line anneal, 1400°F (760°C)/5 min/AC. (500X).....	14
3	Microstructure of low oxygen CORONA 5 after cold-rolling to 0.140 in. (3.5 mm) and annealing 1400°F (760°C)/5 min/AC. (500X).....	15
4	Microstructure of standard oxygen CORONA 5 simulated coil sheet after processing to 0.070 in. (1.8 mm) thickness. (500X).....	16
5	Microstructure of low oxygen CORONA 5 simulated coil sheet after processing to 0.070 in. (1.8 mm) thickness. (500X).....	16
6	Elevated temperature flow stress as a function of strain-rate for both heats of CORONA 5.....	18
7	Strain-rate sensitivity parameter, m, as a function of strain-rate for both heats of CORONA 5.....	19
8	Stress-strain curves as a function of strain-rate at 843°C for low oxygen CORONA 5.....	21
9	Stress-strain curves as a function of strain-rate at 871°C for low oxygen CORONA 5.....	22
10	Stress-strain curves as a function of strain-rate at 898°C for low oxygen CORONA 5.....	23

LIST OF FIGURES

Figure		Page
11	Stress-strain curves as a function of strain-rate at 843°C for standard oxygen CORONA 5	24
12	Stress-strain curves as a function of strain-rate at 871°C for standard oxygen CORONA 5	25
13	Stress-strain curves as a function of strain rate at 898°C for standard oxygen CORONA 5	26
14	Superplastic elongation as a function of temperature at various strain-rates for both heats of CORONA 5	28
15	Typical part shapes produced	30
16	CORONA 5 test parts	31
17	Predicted bond pressure vs bond time for standard oxygen CORONA 5	32
18	Predicted bond pressure vs bond time for low oxygen CORONA 5	33
19	Comparison of predicted bonding parameters for both heats of CORONA 5	34
20	Comparison of predicted bonding parameters and experimental results	36
21	Diffusion bond interfaces as a function of time for low oxygen CORONA 5 bonded at 200 psi (1.38 MPa). (100 and 500X)	37

LIST OF FIGURES

Figure		Page
22	Diffusion bond interfaces as a function of time for low oxygen CORONA 5 bonded at 400 psi (2.76 MPa). (100 and 500X)	38
23	Diffusion bond interfaces as a function of time for low oxygen CORONA 5 bonded at 600 psi (4.14 MPA). (100 and 500X)	39
24	CORONA 5 expanded sandwich part	41
25	Section of expanded sandwich showing truss core configuration	42
26	End view of truss core sandwich part	43
27	Diffusion bond area from truss core sandwich. (100 and 500X)	44

LIST OF TABLES

Table		Page
1	Standard Oxygen CORONA 5 Starting Material	52
2	Low Oxygen CORONA 5 Starting Material	52
3	SPF Forming Study Schedule	53
4	Room Temperature Properties of Simulated CORONA 5 Coil Sheet	54
5	Summary of Tensile Elongation Test Data	55
6	Post-Forming Tensile Results	56

1.0 INTRODUCTION

The alloy Ti-4.5Al-5Mo-1.5Cr (CORONA 5) was originally developed for heavy section, fracture critical applications. The attractive properties exhibited by the alloy have led to studies of using CORONA 5 for advanced fabrication techniques such as superplastic forming (SPF) and diffusion bonding (DB). One such study,[1] indicated that the CORONA 5 alloy is a better candidate from both mechanical behavior and possible economic considerations than the Ti-6Al-4V alloy. Two important cost factors in SPF/DB are cost of sheet production and forming temperature. Essentially all Ti-6Al-4V is produced by a hand sheet process because of the limited cold rollability of this alloy. Production of sheet by a continuous strip process as is used for commercially pure titanium would, potentially, enhance the quality and reduce the cost of alloy sheet. CORONA 5 has been shown to possess good cold rollability[1] and therefore should be a candidate for continuous strip processing. The referenced work also showed that CORONA 5 could be superplastically formed at temperatures below those used for Ti-6Al-4V, a factor that is also economically advantageous. A further potential advantage may be obtained by heat treatment of CORONA 5 to higher strength levels relative to Ti-6Al-4V without requiring a part distorting rapid cooling rate.

The objectives of this program are: (1) to produce fine-grained CORONA 5 sheet by a process amenable to sheet-coil processing, (2) to demonstrate the superplastic formability and diffusion bondability of fine-grained CORONA 5, and (3) to develop post-forming heat treatment schedules that would result in tensile yield strengths on the order of 1035-1105 MPa (150-160 ksi).

The program was conducted by the Rockwell International Science Center and the Crucible Research Center, Colt Industries. Mr. J. C. Chesnutt of the Science Center was the Program Manager and Principal Investigator for the program. Dr. C. H. Hamilton was Co-Principal Investigator at the Science Center. Mr. C. F. Yolton was the Principal Investigator at the Crucible Research Center.

2.0 EXPERIMENTAL PROCEDURES

2.1 Material Processing

Two heats of CORONA 5, a standard oxygen material and a special low oxygen material, were processed during the program. The standard oxygen material was obtained in the form of 3-in. (75 mm) thick plate. This particular plate was produced during a previous NAVAIR Contract.[2] A description of the standard oxygen material is given in Table 1. The low oxygen material, a description of which is given in Table 2, was melted and processed to 1-in. (25 mm) thick plate by TIMET. Both heats were subsequently processed by hot and cold rolling to 0.070 (1.8 mm) thick sheet.

2.1.1 Hot Rolling

The two standard oxygen CORONA 5 plates were hot rolled to hot band gage in two stages. Plates were first heated to 1750°F (954°C) and immediately rolled from 3-in. (75 mm) thick to 0.5-in. (13 mm) thick in 14 passes without reheating. Total elapsed time from leaving the furnace to finish rolling was 1.5 minutes. Approximate finish temperature for each plate was 1300°F (704°C). The material was then reheated to 1650°F (899°C) and rolled to 0.145 in. (3.7 mm) thick. This rolling was accomplished in 5 passes with an elapsed time of 40 seconds for each panel.

The low oxygen material, received as 1-in. (25 mm) thick plate, required only one stage of hot rolling. Before rolling, the as-received plate

was cut into three equal pieces. Heating temperature for this plate was 1650°C (899°C). After attaining a temperature of 1650°F (899°C) the plates were rolled in succession to 0.170-in. (4.3 mm) thick hot band. The rolling was conducted continuously in six passes for each piece within 33-40 seconds to a finishing temperature of 1250°F/1300°F (677°C/704°C).

2.1.2 Cold Rolling

Following processing to hot band gage, all material was cut into convenient size panels for cold rolling. Panels from both heats received a simulated strand line anneal of 1400°F (760°C)/5 minute/air cool. Annealed panels were descaled by grit blasting and then pickled in nitric-hydrofluoric acid solution to remove oxygen contaminated metal. After pickling, the panels were inspected and any surface defects were spot ground. None of the panels were edge trimmed.

The low oxygen hot band finished at a heavier gage than the standard oxygen material. In order to give each material the same amount of final cold reduction, the low oxygen material was cold rolled to the same gage as the standard oxygen hot band. Following the 16% reduction, the low oxygen material was annealed 1400°F (760°C)/5 minutes/air cool, descaled and pickled.

Material from both heats was given a final cold reduction of approximately 48% to 0.073 (1.8 mm) thick. After the final cold reduction all material was again given a simulated strand line anneal of 1400°F (760°C)/5 minutes/air cool, descaled and pickled in nitric-hydrofluoric acid solution.

Throughout all hot and cold rolling, the original plate rolling direction was maintained for each material. A limited amount of testing was conducted on each material after processing as reported in Section 3.1.

2.2 Tensile Tests

The two heats of the CORONA 5 material containing standard oxygen and low oxygen contents were tested at elevated temperatures for superplastic properties. Tensile tests were conducted at temperatures of 834, 871 and 899°C (1550, 1600 and 1650°F). The testing included step/strain-rate tests for the determination of the flow stress as a function of strain rate, and corresponding determination of the strain-rate sensitivity exponent, m, as a function of strain rate. The test procedures utilized here were the same as those reported in Ref. 3. Properties established in these step/strain rate tests were for relatively low strain levels of less than about 0.25 total strain and therefore, subsequent tests were also conducted under constant strain-rate conditions to establish the influence of strain on flow stress and on the m value. The test specimens, on which the constant strain-rate tests were conducted, were tested to failure so that the total elongation under superplastic conditions could also be established.

The tensile tests for the evaluation of these superplastic properties were conducted under vacuum conditions through the use of a specially equipped Instron test machine. The heating was accomplished with a five zone furnace so that the temperature gradients could be maintained within about ±2°C. The Instron machine was adapted such that constant strain-rate could be

established through the use of the variable speed motor connected through the drive train of the equipment. This variable speed motor was controlled by programmed electronic profiling devise (Versatrac). The test specimens used in this test consisted of the 1 in. gage section and were a "dog-bone" configuration which were pin loaded in the end sections. All test specimens were machined such as the long transverse orientation was coincident with the tensile test direction.

2.3 Forming Tests

The superplastic formability of the CORONA 5 materials was evaluated through the subscale superplastic forming tests conducted on the sheet materials. These tests involved the forming of rectangular and cylindrical part configurations. Both the low oxygen and the standard oxygen materials were evaluated although the majority of the forming tests were conducted on the low oxygen materials because of the evidence that these materials exhibited the best superplastic properties at the elevated temperatures. The forming tests were conducted utilizing tooling machined from an iron-base tooling alloy containing 22% Cr, 4% Ni and 9% Mn. The gas pressure application was controlled in such a fashion as to attempt to control the strain-rate throughout the forming test using methods such as those described in Ref. 4. These analytical techniques, utilized to predict pressure as a function of time for strain-rate control, have been found to be quite good for specific configurations such as the rectangular pan sections and the cylindrical parts evaluated in this study. In these forming tests, argon gas was utilized both as the

forming medium and as protective gas cover on the sheet to be superplastically formed. This technique, used throughout industry for several years, is reported in more detail in Ref. 5.

The forming tests involved varying both the forming temperature and the strain rate in addition to the alloy composition. A summary of the forming parameters evaluated are presented in Table 3. The forming parameters utilized in this study are based on the tensile test results established through the evaluations described in Section 2.2. Some of the parts formed during this task were sectioned to provide tensile specimens for the post-forming heat treatment study reported in Section 2.6.

2.4 Diffusion Bonding Tests

The diffusion bonding of titanium alloys depends primarily on their elevated temperature flow properties.[6-8] The analytical models of Refs. 6 and 7 provide excellent predictions of the pressure versus time combinations necessary to achieve intimate contact along a diffusion bond interface and thus complete bonding in Ti alloys. The material property considered in these models is primarily the flow stress of the material as a function of the strain-rate imposed. Since such data were generated under Section 2.2 of this report it was possible to predict analytically the diffusion bond pressures required as a function of time for the various materials and temperatures of concern.

In addition to the analytical predictions, an experimental evaluation test program was conducted to verify the diffusion bond parameters for the low oxygen heat material at 871°C (1600°F). In these tests three different bond pressures were evaluated as a function of time. Samples of the sheet material measuring approximately 1 in. × 1 in. (25.4 mm × 25.4 mm) in plan area were diffusion bonded under conditions of vacuum of less than 10^{-4} torr (13.3 mPa) at the temperature of 871°C. These samples were then evaluated metallographically for quality of the diffusion bond interface and for evidence of porosity at the bond interface. The diffusion bonding parameters were chosen to bracket the predicted bond pressures required in order to provide a verification that these predicted parameters were correct.

2.5 SPF/DB Fabrication Demonstration

As a final demonstration of the potential for combining superplastic forming with diffusion bonding of the CORONA 5 alloy, a fabrication demonstration was conducted to produce a truss-core sandwich configuration utilizing the low oxygen heat of the CORONA 5 alloy. This sandwich consisted of flat sheets of the CORONA 5 alloy in which the center sheet providing the material for the core of the sandwich was 0.029 in. (0.7 mm) thick and the two face sheets were the outer sheets of the sandwich were approximately 0.070 in. (1.8 mm) thick.

The stop-off pattern was applied to the core sheet using techniques that had been established for the SPF/DB Ti technology as reported in Ref. 8. Stop-off material utilized in this case was yttria which was applied by silk-screening method as described in Ref. 8. Three sheets of material were

placed in a die at ambient temperatures and the die was used for both diffusion bonding and subsequent superplastic forming. Capillary tubes were inserted into the two ends of the sandwich panel prior to the heat-up of the material to facilitate superplastic expansion subsequent to diffusion bonding. The tooling was then heated to a temperature of 871°C (1600°F) for both the diffusion bonding and superplastic forming. Once the temperature was achieved, the gas pressure was applied to the bottom side of the layer and forced the three sheets together providing the pressure for diffusion bonding. The diffusion bonding parameters chosen were 400 psi (2.76 MPa) for a time of 75 minutes. These parameters were chosen on the basis of the experimental results conducted as discussed in Section 2.4.

After the diffusion bonding cycle was completed, the gas pressure on the bottom side of the panel was released and the forming gas pressure was introduced through the capillary tubes between the sheets of the CORONA 5. Introduction of gas pressure between the the sheets initiated the superplastic forming portion of the cycle causing the face sheets to form into the surrounding die cavity. The strain-rate during this part of the forming cycle was controlled at $\sim 2 \times 10^{-4}$ s^{-1}, a strain-rate that was found to be nearly optium for this material in terms of generating a high degree of superplasticity. This fabrication test, based upon the parameters established from the tensile tests, forming tests, and the diffusion bonding tests, was a demonstration that the parameters established in the previous tests were adequate for establishing the SPF/DB processing conditions and parameters.

2.6 Post-Forming Heat Treatment

A study of the heat treatment response of sheet both prior to and subsequent to superplastic forming was conducted. Tensile property evaluation of sheet material included the following conditions:

1. Cold-rolled plus annealed (CR+A)

2. CR+A plus simulated DB cycle [1600°F (871°C)/2 hr/AC]

3. CR+A plus simulated DB cycle plus aged [1050°F (566°C)/8 hr/AC]

4. CR+A plus formed

5. CR+A plus formed plus solution treated and aged.

Heat treatments were chosen on the basis of Ref. 1 and ongoing heat treatment studies in a companion program.[9] Due to a scarcity of low oxygen sheet material, heat treatment studies for this heat were limited to specimens removed from formed pans that correspond to conditions 4 and 5 above. Small "dog-bone" tensile specimens were removed from the sides and bottom of formed pans of both heats of material. The tensile axis of the specimen corresponds to the long axis of the pan and the sheet rolling direction (RD or L). Specimens had a 1 in. (25.4 mm) gage length and a cross section of 0.25 in. (6.4 mm) by sheet thickness. Specimen thickness may have varied due to non-uniform

thinning in the pan; a mid gage-length thickness was used in the stress calculations. All heat treatments were conducted in a vacuum of 10^{-6} torr (0.133 mPa) or better and the specimens were wrapped in tantalum foil to further reduce contamination. Following heat treatment the specimens were lightly pickled in a nitric-hydrofluoric acid solution prior to test. All tests were conducted at a strain rate of approximately 10^{-4} s^{-1}.

3.0 RESULTS AND DISCUSSION

3.1 Material Characterization

The scope of the program did not allow a significant amount of material evaluation, however, a limited test program was conducted to determine basic sheet properties.

Microstructure of the as-hot rolled hot band is shown in Fig. 1. In both materials this structure is relatively fine and grain elongation in the rolling direction is evident. Figure 2 shows the microstructure of the standard grade material after a simulated stand line anneal. The anneal did not produce a significant change in the hot rolled structure; the microstructure of the low oxygen material after the first cold reduction and anneal is shown in Fig. 3. The 16% cold reduction produced a significant amount of recrystallization in the low oxygen material. Microstructures of the two heats after processing to 0.070 in. (1.8 mm) thick annealed sheet, are shown in Figs. 4 and 5. Both materials exhibit very fine grained structures which cannot be fully resolved in the optical microscope.

Mechanical properties determined for the simulated CORONA 5 coil sheet were monotonic tensile properties, bend ductility and Olsen Cup formability. Results are given in Table 4. In general, the strengths are higher and the tensile ductilities lower than typical properties of Ti-6Al-4V sheet. The CORONA 5 sheet also shows a substantial amount of strength directionality. Room temperature formability, as measured by bend and Olsen cup tests, is better than the Ti-6Al-4V alloy. Since this material was to be

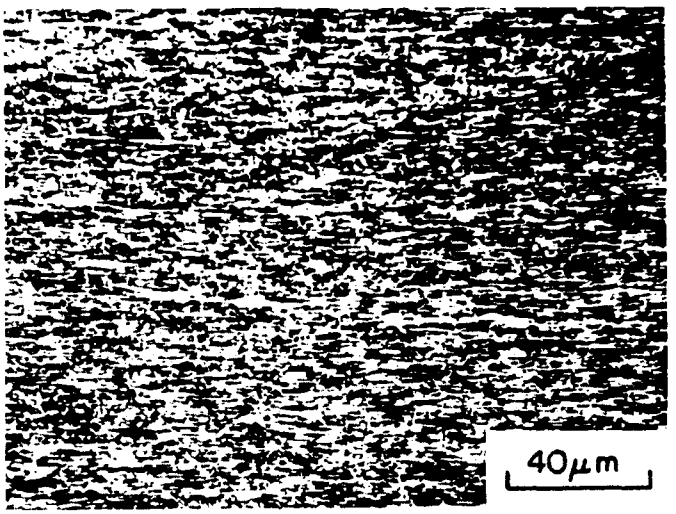

STANDARD OXYGEN MATERIAL

LOW OXYGEN MATERIAL

Fig. 1 Microstructure of as-hot rolled CORONA 5 hot band. (500X)

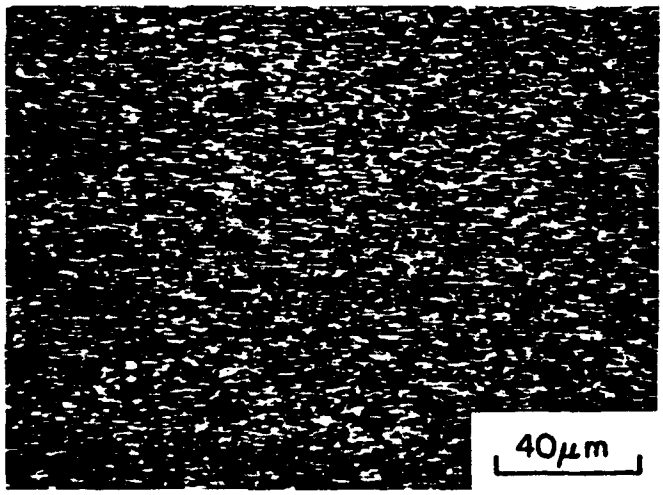

Fig. 2 Microstructure of standard oxygen CORONA 5 hot band after a simulated strand-line anneal, 1400°F (760°C)/ 5 min/AC. (500X)

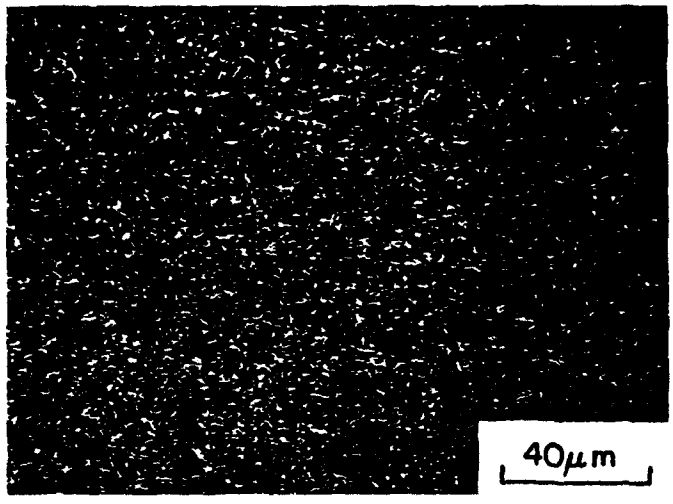

Fig. 3 Microstructure of low oxygen CORONA 5 after cold-rolling to 0.140 in. (3.5 mm) and annealing 1400°F (760°C)/5 min/AC. (500X)

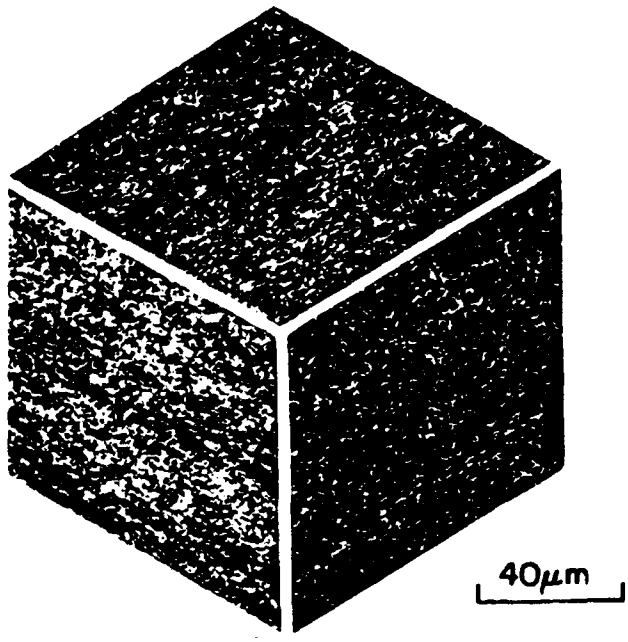

Fig. 4 Microstructure of standard oxygen CORONA 5 simulated coil sheet after processing to 0.070 in. (1.8 mm) thickness. (500X)

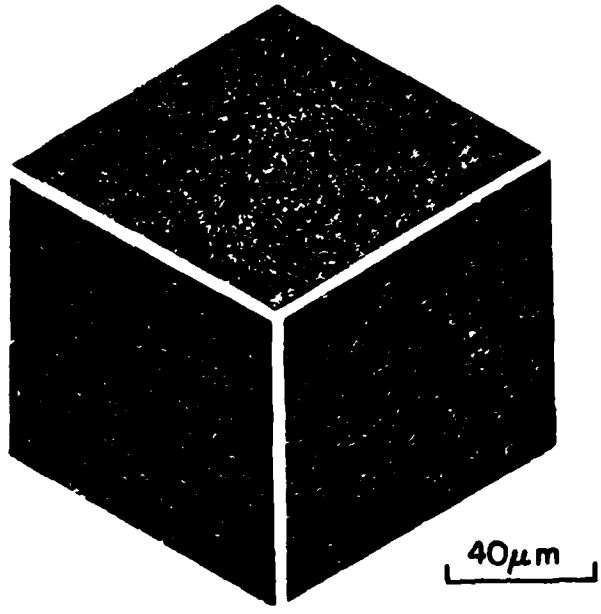

Fig. 5 Microstructure of low oxygen CORONA 5 simulated coil sheet after processing to 0.070 in. (1.8 mm) thickness. (500X)

superplastically formed and hence receive a high temperature thermal exposure, the strand line anneal tensile properties are not of particular importance to the program. However, if material were to be used in the annealed condition, modifications could be made in the processing to reduce directionality and increase ductility.

In order to ensure that no interstitial contamination had occurred during processing of the sheet, oxygen and hydrogen analyses were conducted on the finished material. These results are also given in Table 4. Results indicate no oxygen or hydrogen pickup occurred during processing.

3.2 Tensile Tests

The results of the elevated temperature tensile tests in which the flow-stress as a function of strain-rate and m as the function of strain-rate were evaluated are shown in Figs. 6 and 7. As can be seen in these figures the flow-stresses for the various materials and temperatures evaluated vary from one another only marginally, although it appears that the lower flow-stresses occur for the low oxygen alloy material. It is also apparent from the Figs. 6 and 7 that the temperatures of 843 and 871°C are better suited for superplasticity for this alloy than 898°C where the flow-stresses are higher and the strain-rate sensitivity appears to be somewhat less. In reference to Fig. 7 it appears that the m value is increasing as the strain-rate decreases to a strain-rate of approximately 10^{-5} s^{-1}. For other Ti alloys it has been observed that the m value reaches a maximum and then decreases at lower strain-rates, and therefore it is likely that the maximum in m for this

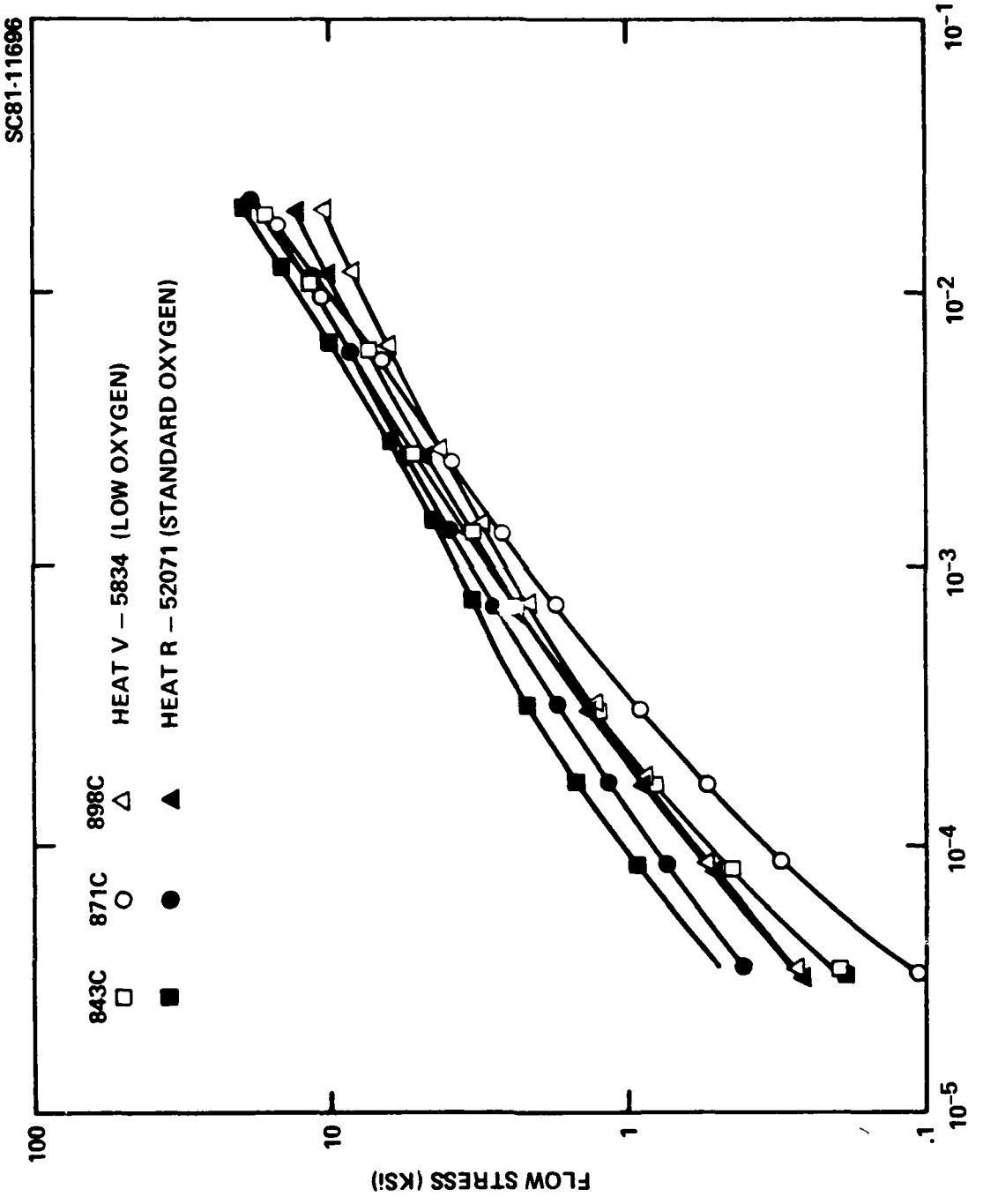

Fig. 6 Elevated temperature flow stress as a function of strain-rate for both heats of CORONA 5.

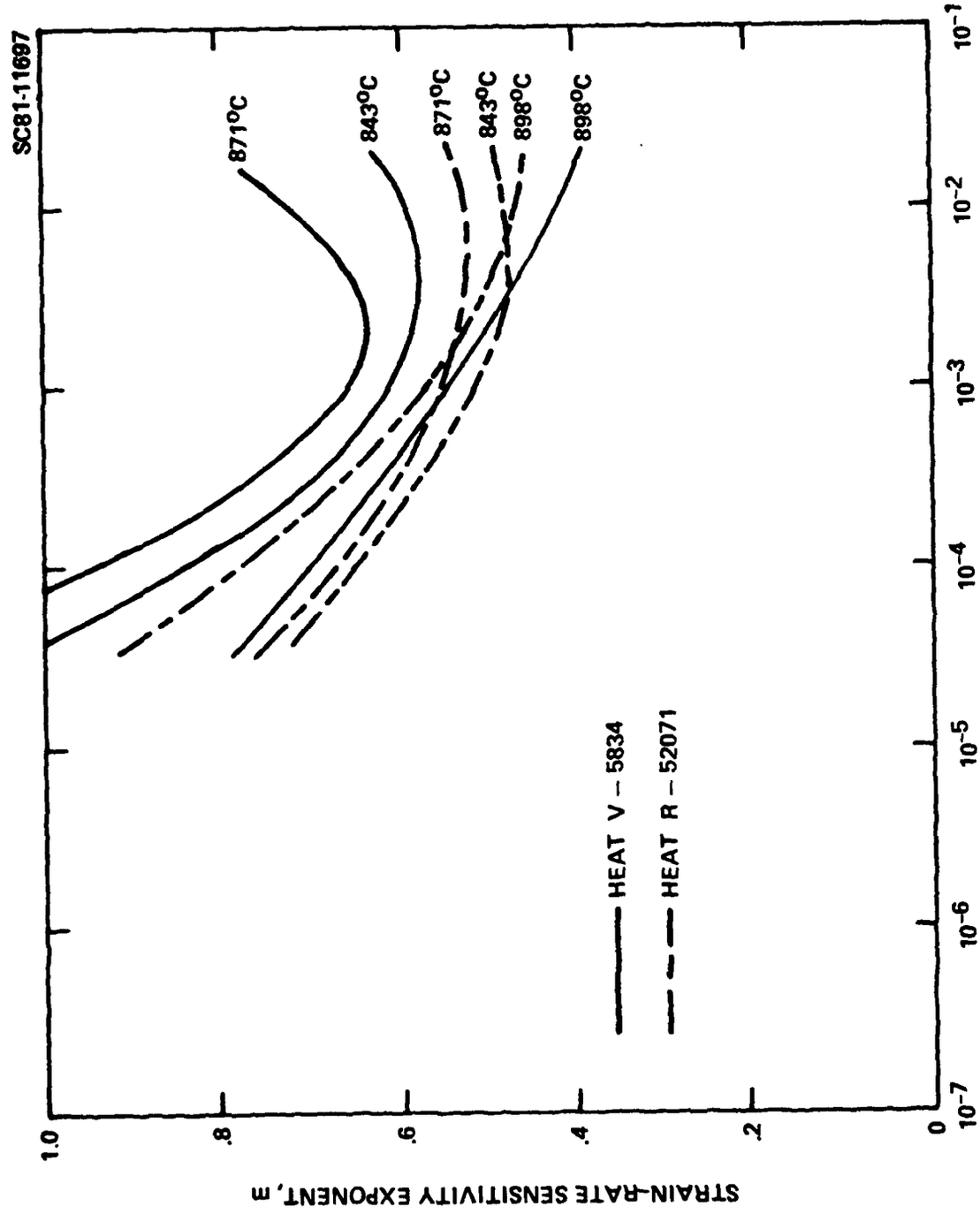

Fig. 7 Strain-rate sensitivity exponent, m, as a function of strain-rate for both heats of CORONA 5.

material occurs at strain-rates lower than those evaluated in this program. The strain-rate sensitivity exponent, m, continues to decrease as the strain-rate increases to strain-rates of about 10^{-3} s^{-1} and above. In some cases the m value appears to rise slightly at strain-rates above about 5×10^{-3} to 10^{-2} s^{-1}. It is considered likely, however, that this increase is primarily a result of a rapid strain-hardening in the material at the very high strain rates rather than an increasing m. This is likely to occur since the material tested is exposed to the lower strain-rates first and then exposed to higher strain-rates at correspondingly higher strain levels. Thus, any strain hardening would result in higher flow stresses in the material which could be reflected in higher m values.

The results of these tests reveal that the low oxygen content material exhibits somewhat lower flow-stresses than the standard oxygen material, and in fact the lowest flow-stresses and highest m values observed were at 1600°F (871°C) for the low oxygen material.

The results of the constant strain rate tests at temperatures 843°C, 871°C, and 898°C are shown in Figs. 8 through 10 for the low oxygen material and in Figs. 11 through 13 for the standard oxygen material. These data support the observation that, particularly at the lower temperatures, the flow-stresses for the low oxygen alloy are somewhat less than for the standard oxygen content material. Some strain-hardening can be observed, particularly for the lower flow stress materials at the various temperatures, and it appears that the strain-hardening is greater at temperatures of 871°C and 898°C than at the lower temperature of 843°C. A probable reason for this is a

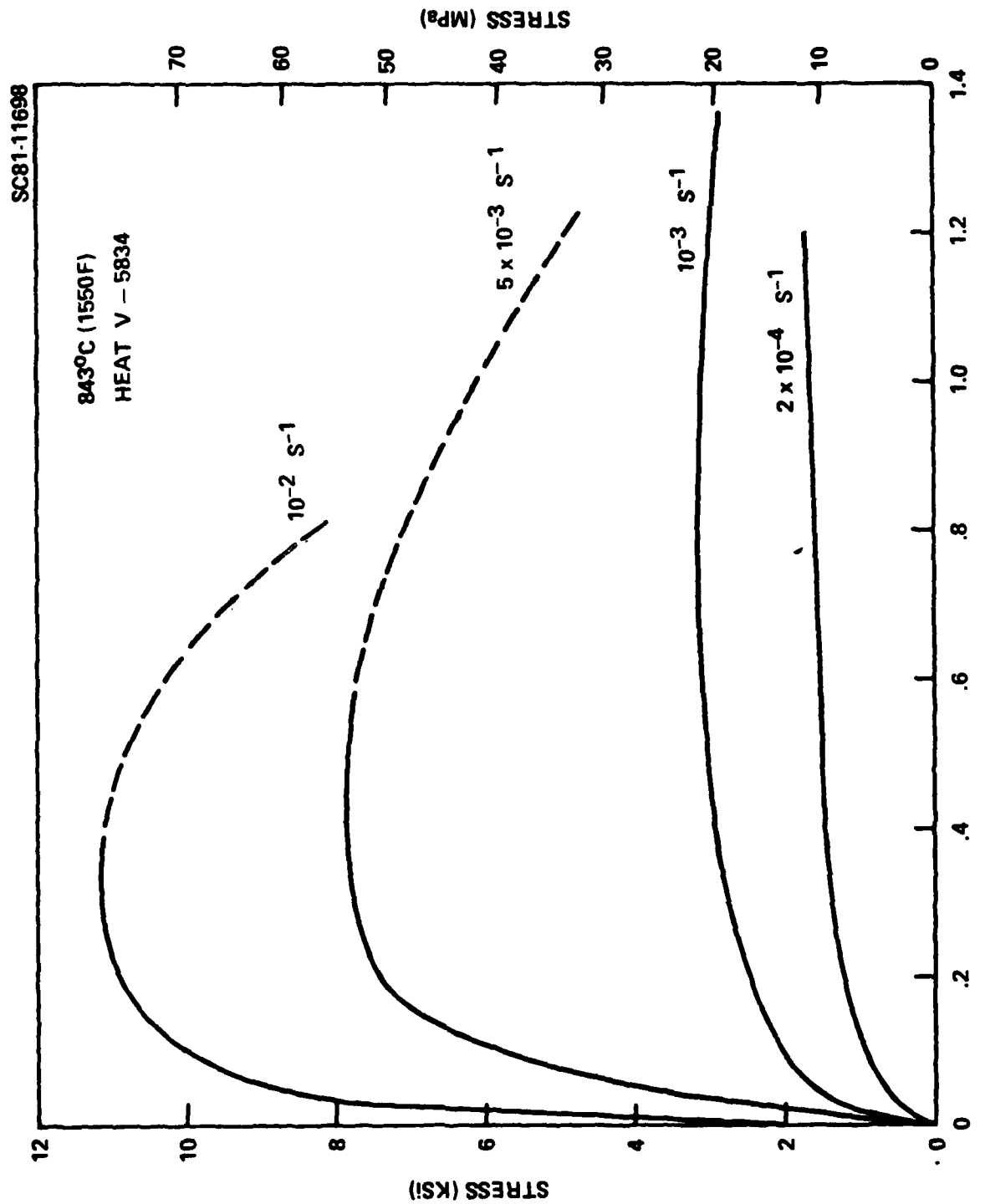

Fig. 8 Stress-strain curves as a function of strain-rate at 843°C for low oxygen CORONA 5.

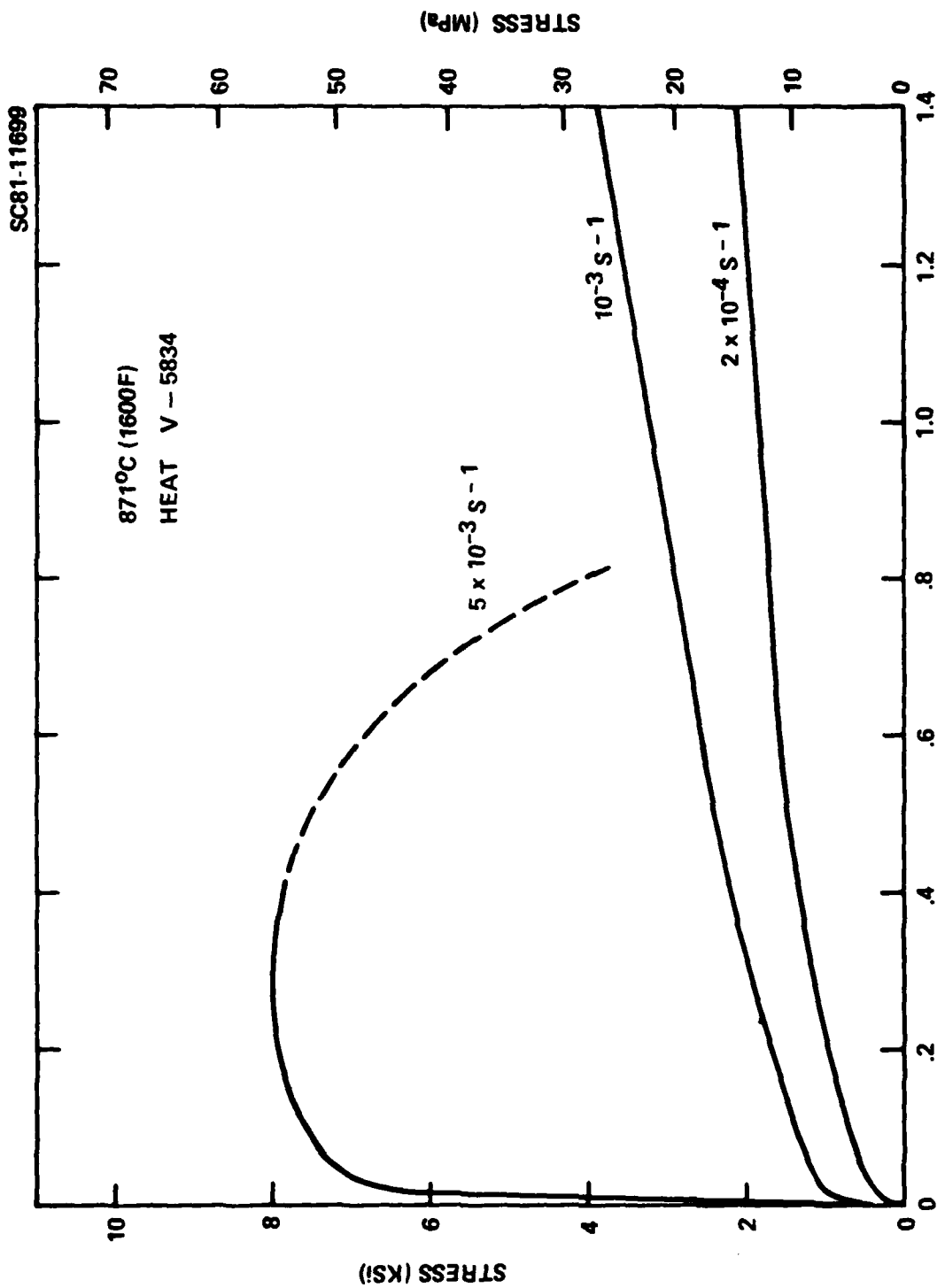

Fig. 9 Stress-strain curves as a function of strain-rate at 871°C for low oxygen CORONA 5.

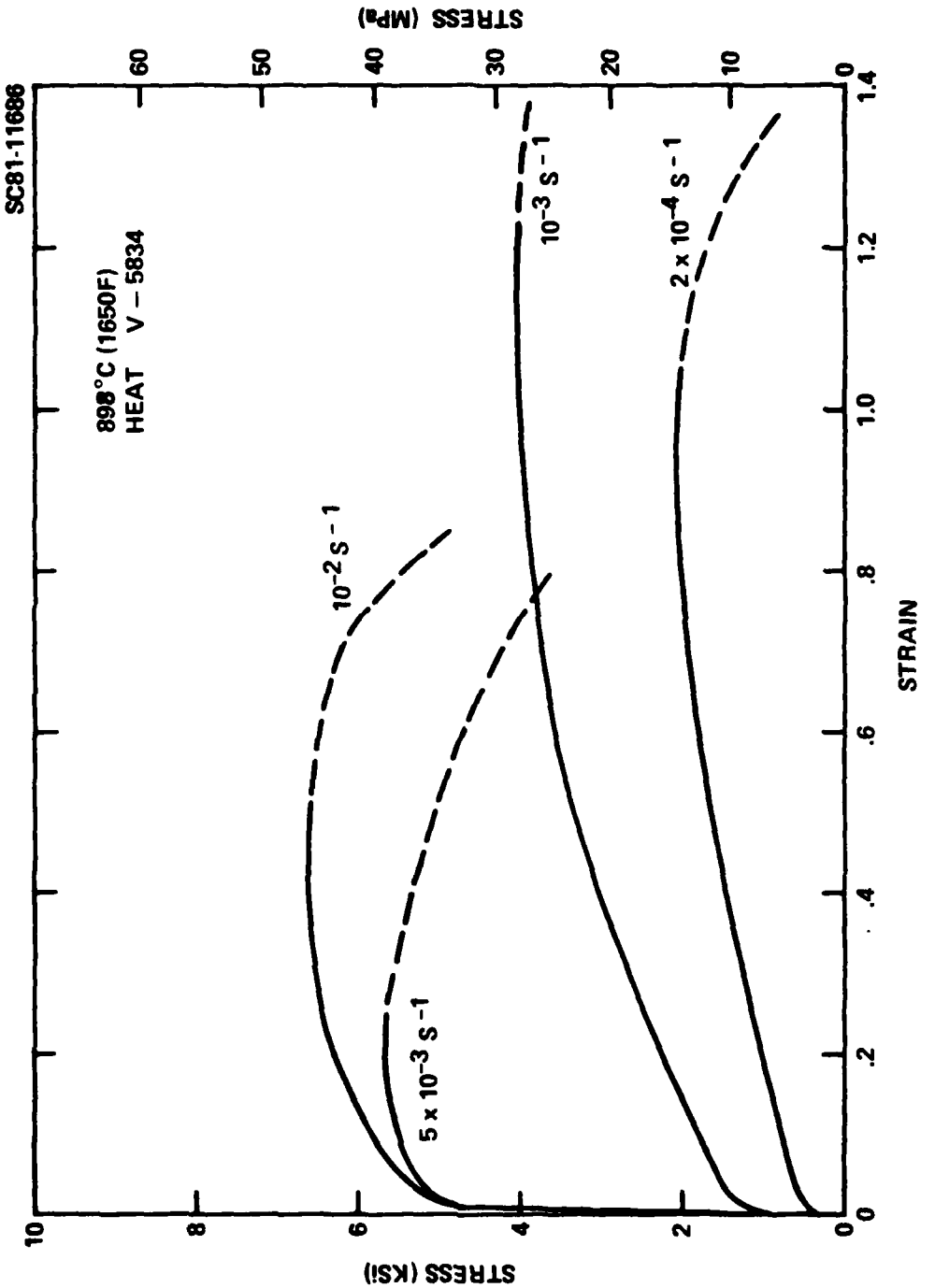

Fig. 10 Stress-strain curves as a function of strain-rate at 898°C for low oxygen CORONA 5.

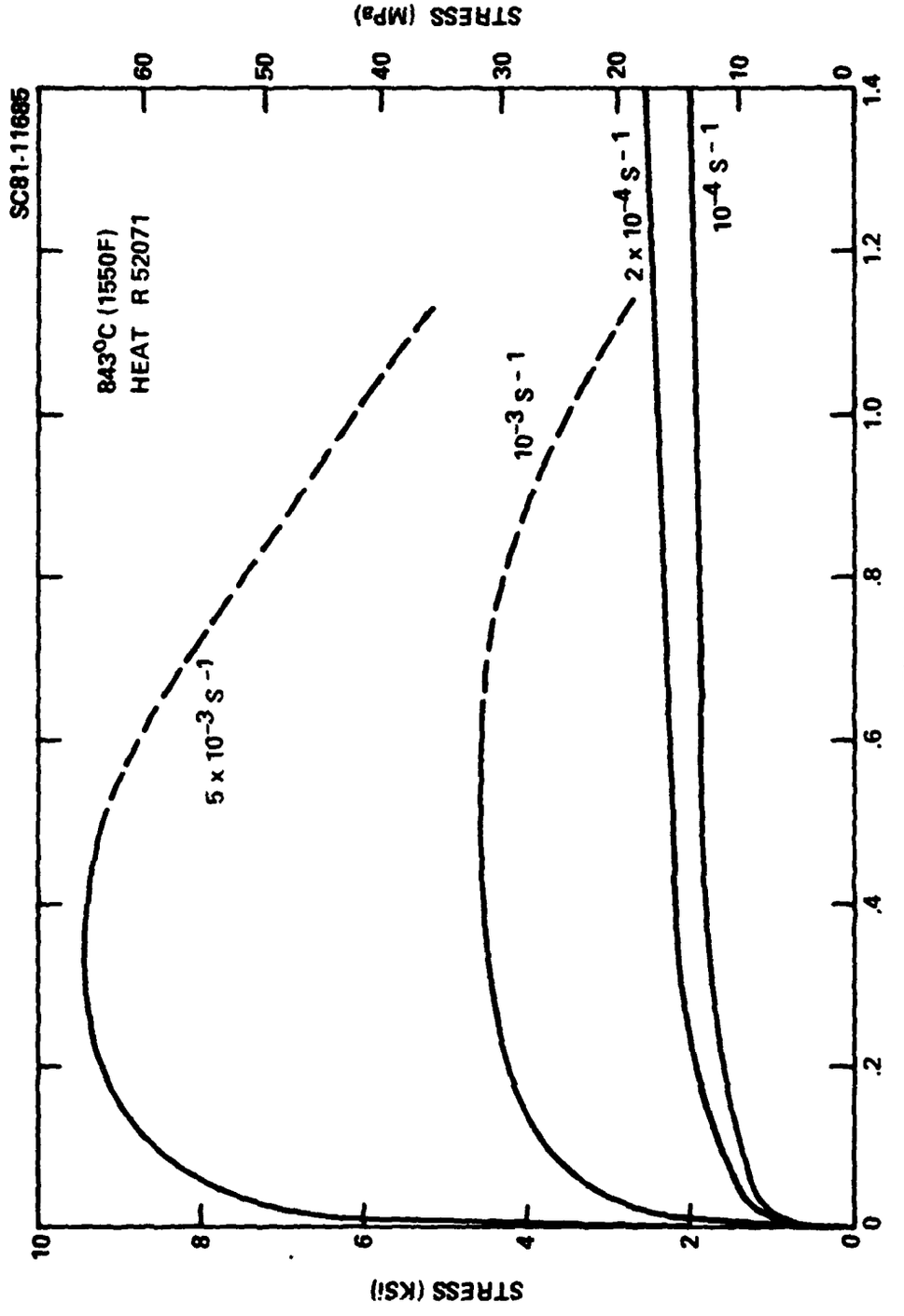

Fig. 11 Stress-strain curves as a function of strain-rate at 843°C for standard oxygen CORONA 5.

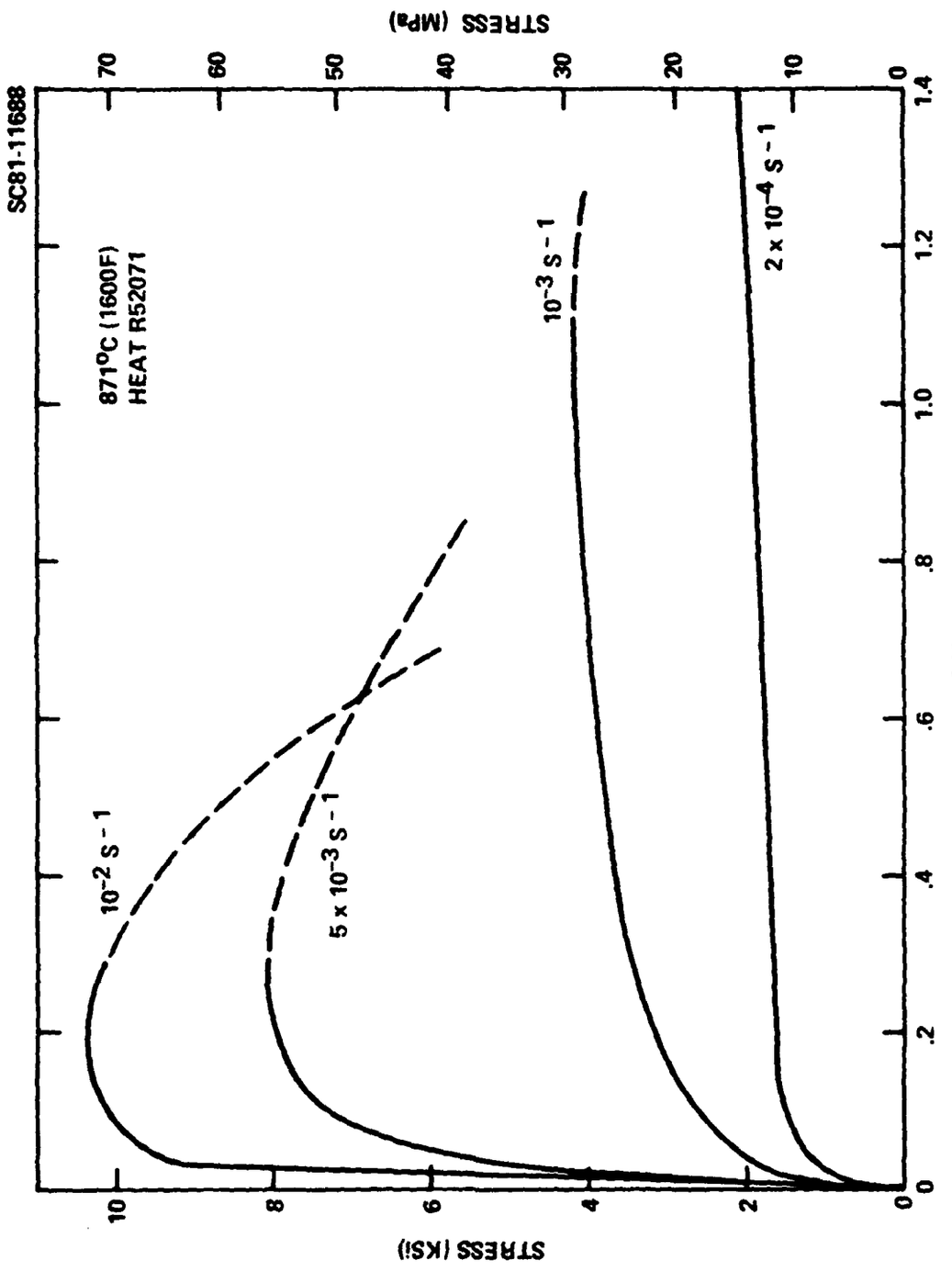

Fig. 12 Stress-strain curves as a function of strain-rate at 871°C for standard oxygen CORONA 5.

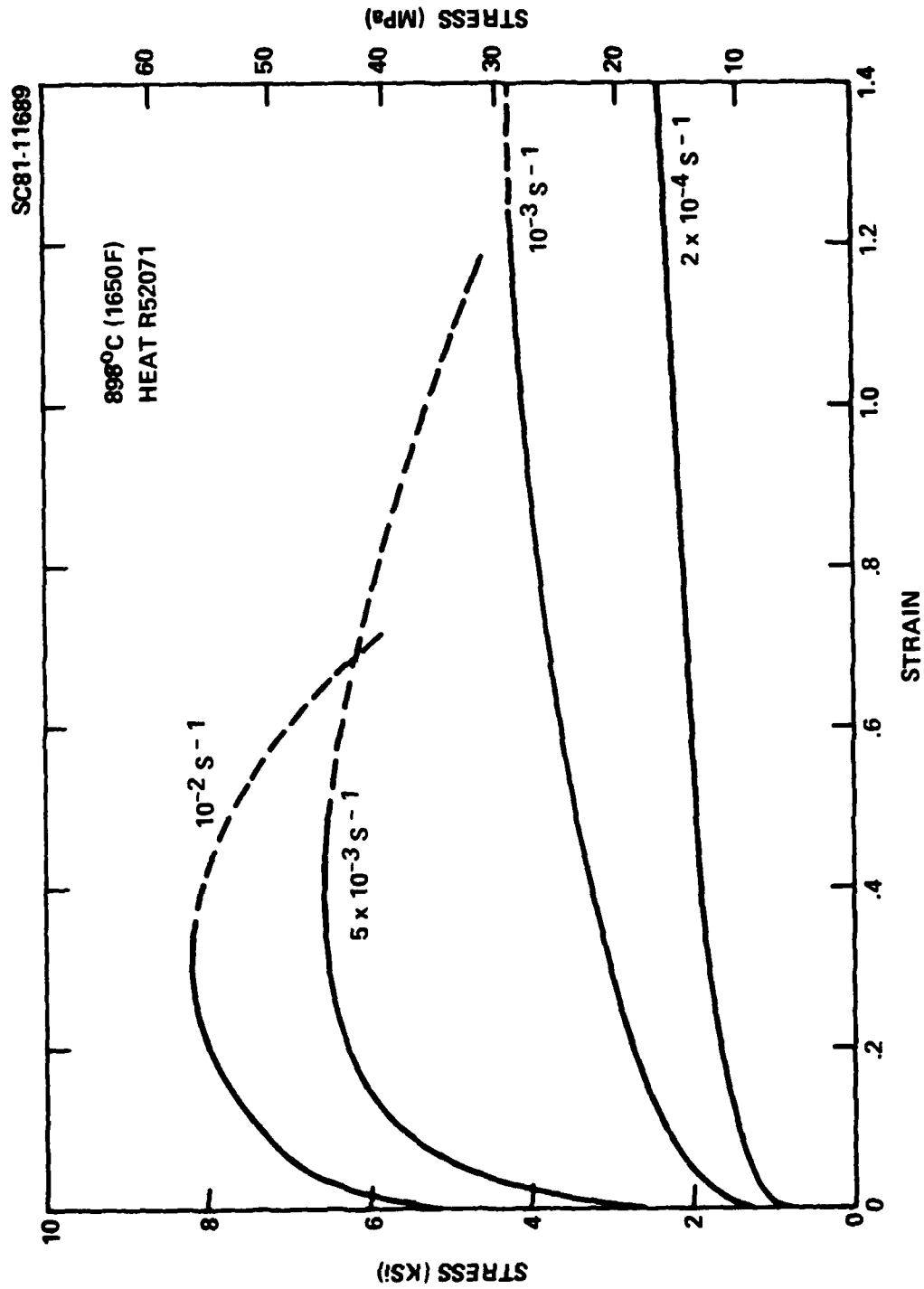

Fig. 13 Stress-strain curves as a function of strain rate at 898°C for standard oxygen CORONA 5.

difference in the grain coarsening kinetics for these temperatures that influence the flow stress of the material (as has been reported for the Ti-6Al-4V alloy in Ref. 3). The data suggests that the optimum superplastic properties would be observed within the 843 to 871°C temperature range rather than at higher temperatures. For conditions where long exposure times at high temperatures are necessary, the low temperature (843°C) may be preferable to the intermediate and higher temperatures.

The results of the total elongation tests at the various temperatures and strain-rates are summarized in Table 5 and are shown graphically in Fig. 14. These data indicate the optimum superplastic temperature is approximately 871°C and that superplasticity appears to decrease substantially above this. The total elongations observed for the CORONA 5 alloy at 871°C exceed approximately 500% tensile elongation. However, even for the lower temperature of 843°C, total elongation values of 400-500% are observed, and this ductility is sufficient for superplastic forming of a large number of structural components. In Table 5, the strain-rate sensitivity exponent, m, is also shown and it is apparent that this value correlates approximately with the total elongation measurements, a characteristic that has been reported many times for superplastic materials.

3.3 Forming Tests

The optimum parameters for superplastic forming sheet materials based on the tensile tests discussed previously are 871°C and below to 843°C. The superplastic forming of the CORONA 5 was conducted within this temperature

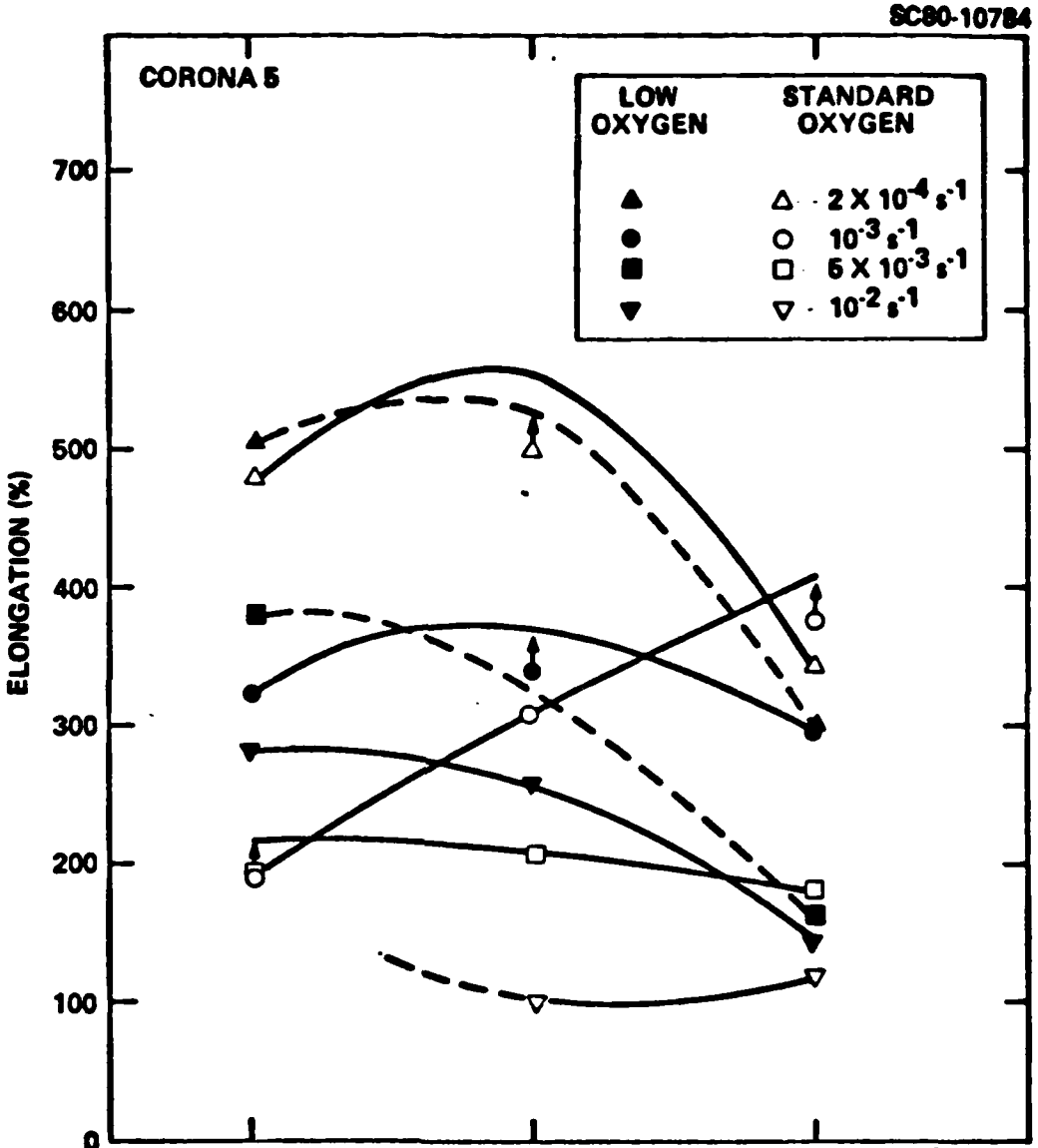

Fig. 14 Superplastic elongation as a function of temperature at various strain-rates for both heats of CORONA 5.

range and for the higher temperature as well. The rectangular pan configuration was the configuration used to demonstrate the formability at temperatures of 843, 871 and 899°C. In addition, a cylindrical part which imposed the maximum balanced biaxial straining for superplastic forming was formed at 871°C. A deep rectangular part was formed at 871°C to demonstrate severe forming under plain strain conditions. (See Fig. 15 for an illustration of the forms produced).

Forming of all of these shapes proceeded without difficulty and the resulting parts verified the superplastic formability of both the standard oxygen and the low oxygen CORONA 5. The series of superplastically formed CORONA 5 test parts are shown in Fig. 16. Strains that were developed in these subscale components are at least equivalent to and in many cases exceed, the strain levels encountered in many of the superplastically formed parts produced from the Ti-6Al-4V alloy. The rectangular components shown in Fig. 16 were the superplastically formed parts that were subjected to past forming tensile test evaluation reported in Section 3.6.

3.4 Diffusion Bonding Tests

The results of the analytical predictions of the bonding parameters are summarized in Figs. 17 through 19. In Fig. 17, the predicted bond pressure as a function of bond time is shown for the standard oxygen material for the three temperatures indicated. For the low oxygen material similiar plots are shown in Fig. 18. It is apparent in comparing these two figures that the low oxygen material would be expected to require somewhat lower bonding

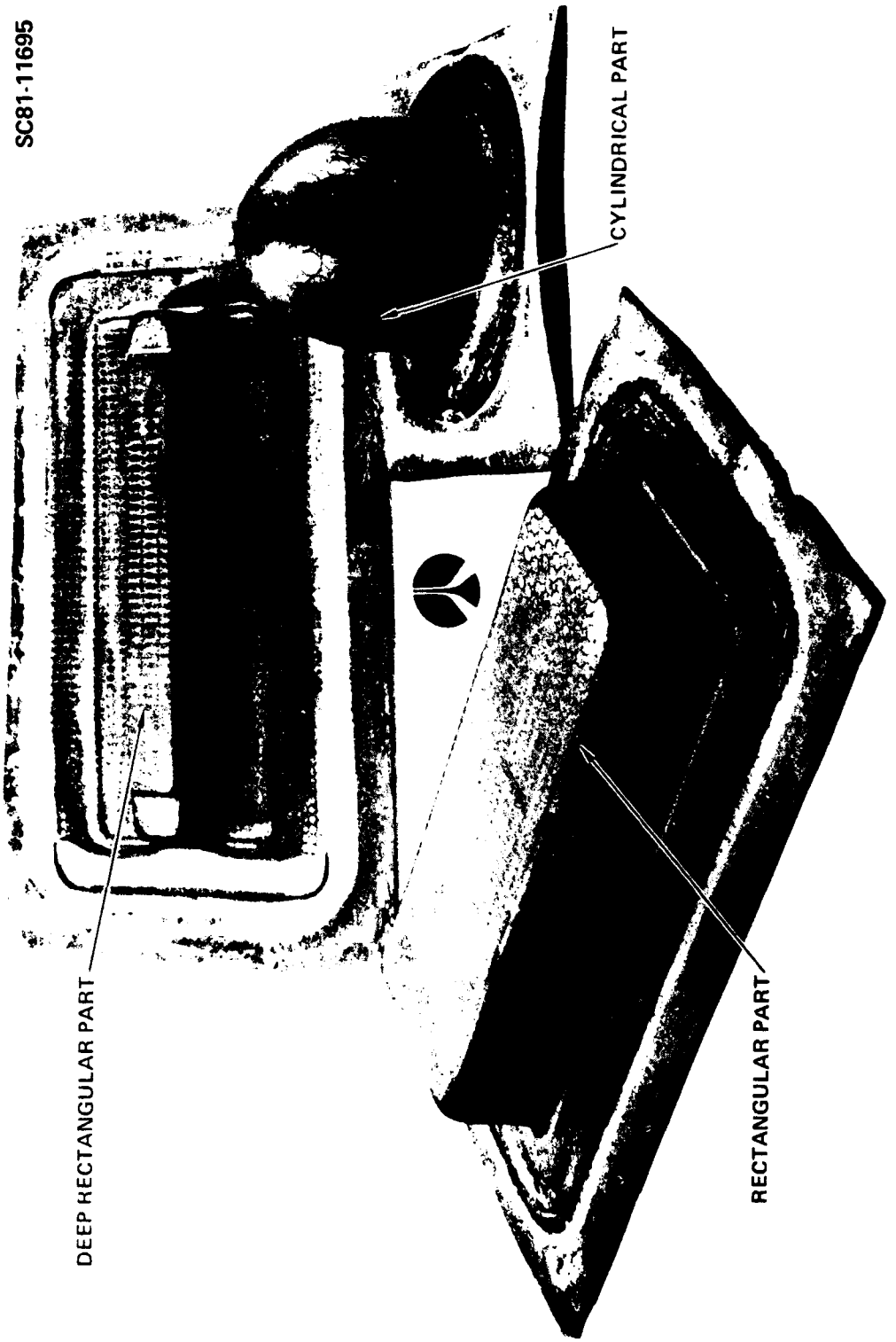

Fig. 15 Typical part shapes produced.

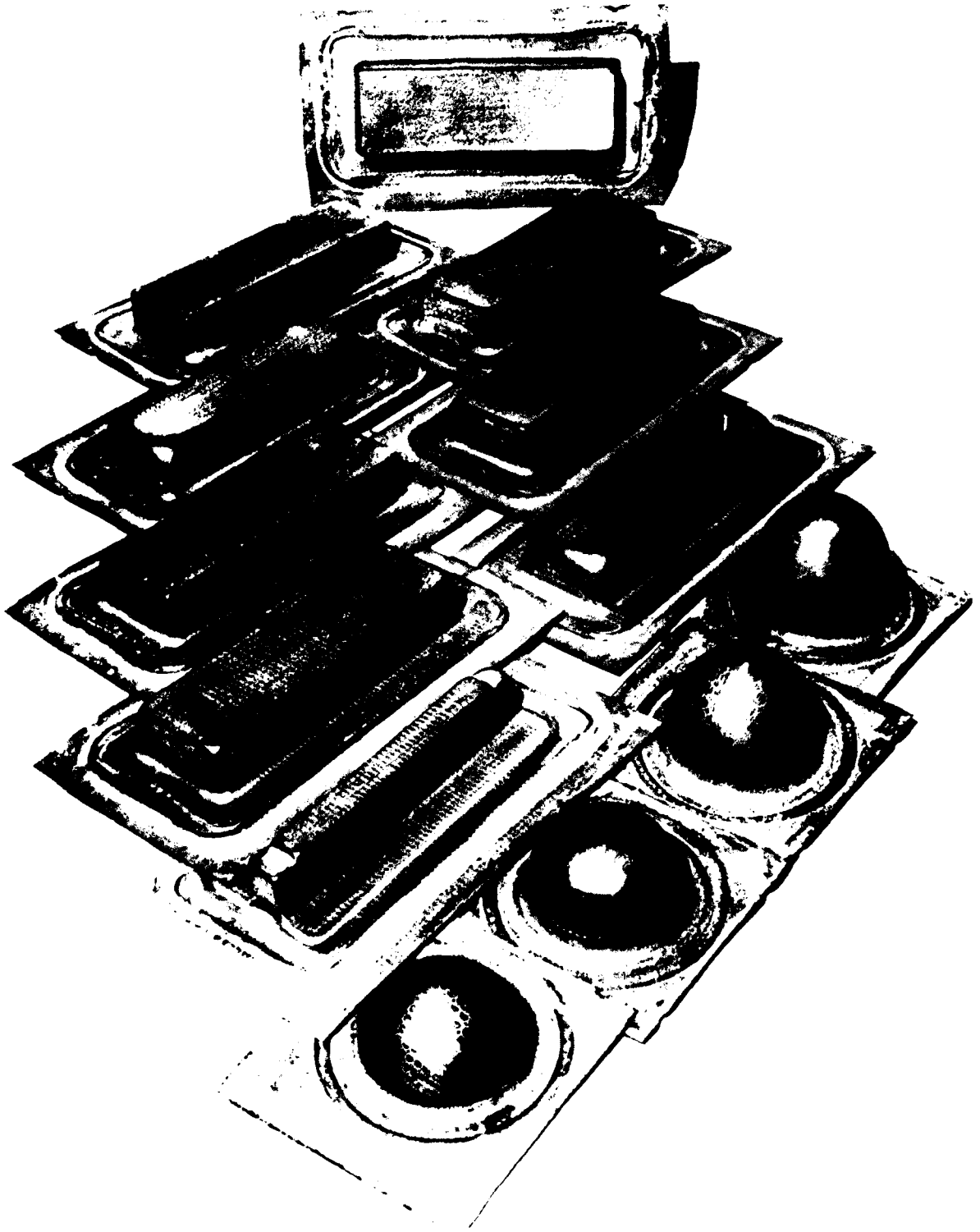

Fig. 16 CORONA 5 test parts.

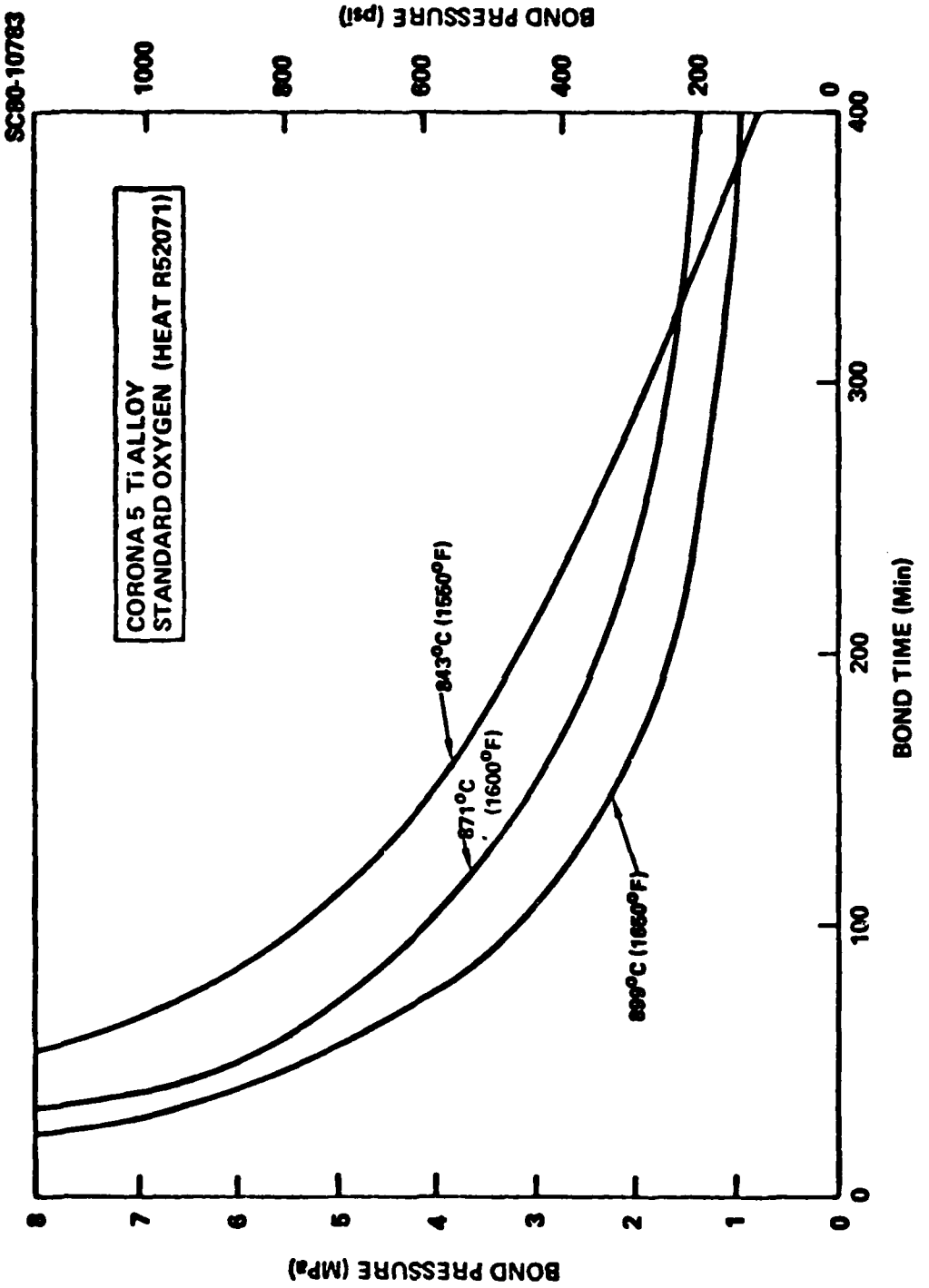

Fig. 17 Predicted bond pressure vs bond time for standard oxygen CORONA 5.

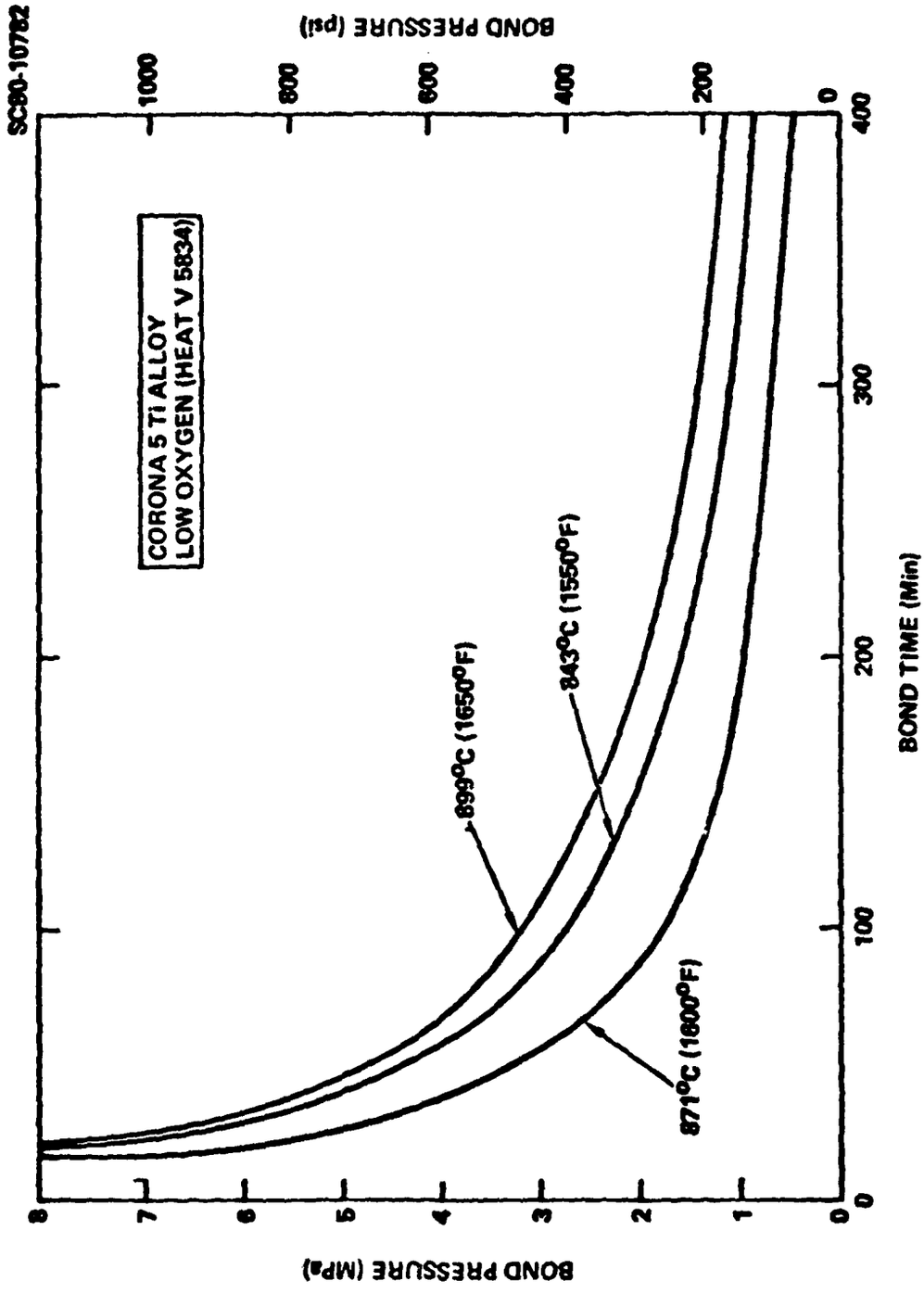

Fig. 18 Predicted bond pressure vs bond time for low oxygen CORONA 5.

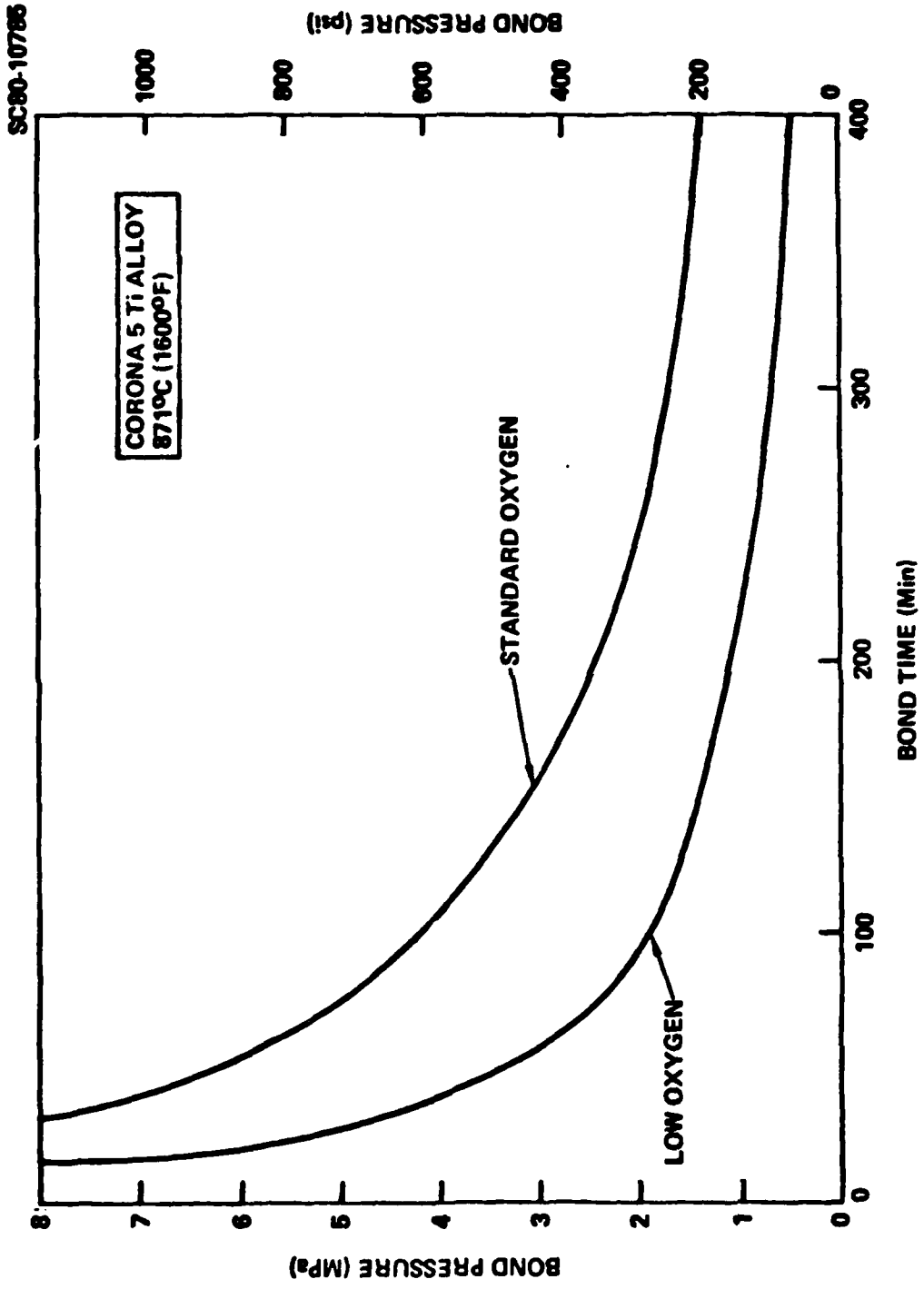

Fig. 19 Comparison of predicted bonding parameters for both heats of CORONA 5.

pressures than the standard oxygen material, although the bonding parameters required for the standard oxygen material are sufficiently low that it should be possible to use gas pressure diffusion bonding. For the low oxygen material (Fig. 18), the bonding pressures appear to be minimized at 871°C, while for the standard oxygen material, bonding pressures appears to be minimized at 899°C. A comparison of the standard and low oxygen materials for temperature of 871°C is shown in Fig. 19. In this figure it is apparent that the low oxygen material requires much lower diffusion bonding pressure than does the standard oxygen material at this temperature.

Since these curves are established analytically, it was the intent of the experimental study to verify that these curves provided a reasonable indication of the bonding parameters for this material. The low oxygen heat of the material was selected for the diffusion bonding, and the bonding study was conducted at 871°C and for times that bracketed the predicted times for bonding. The experimental results are presented along with the analytical prediction in Fig. 20. In this figure it can be seen that the experimental results suggest that, although the predicted curve is quite close to experimental observation, a modification of this curve would more closely represent the actual results. Therefore, in this figure the dotted curve represents the experimental results and more closely predicts the diffusion bonding parameters for this heat of material. These results do not modify the conclusions that relatively low bonding pressures can be used to diffusion bond low oxygen CORONA 5. The diffusion bond interfaces for various bonding parameters (pressure and time) at 871°C are shown in Figs. 21, 22, and 23. Porosity at the

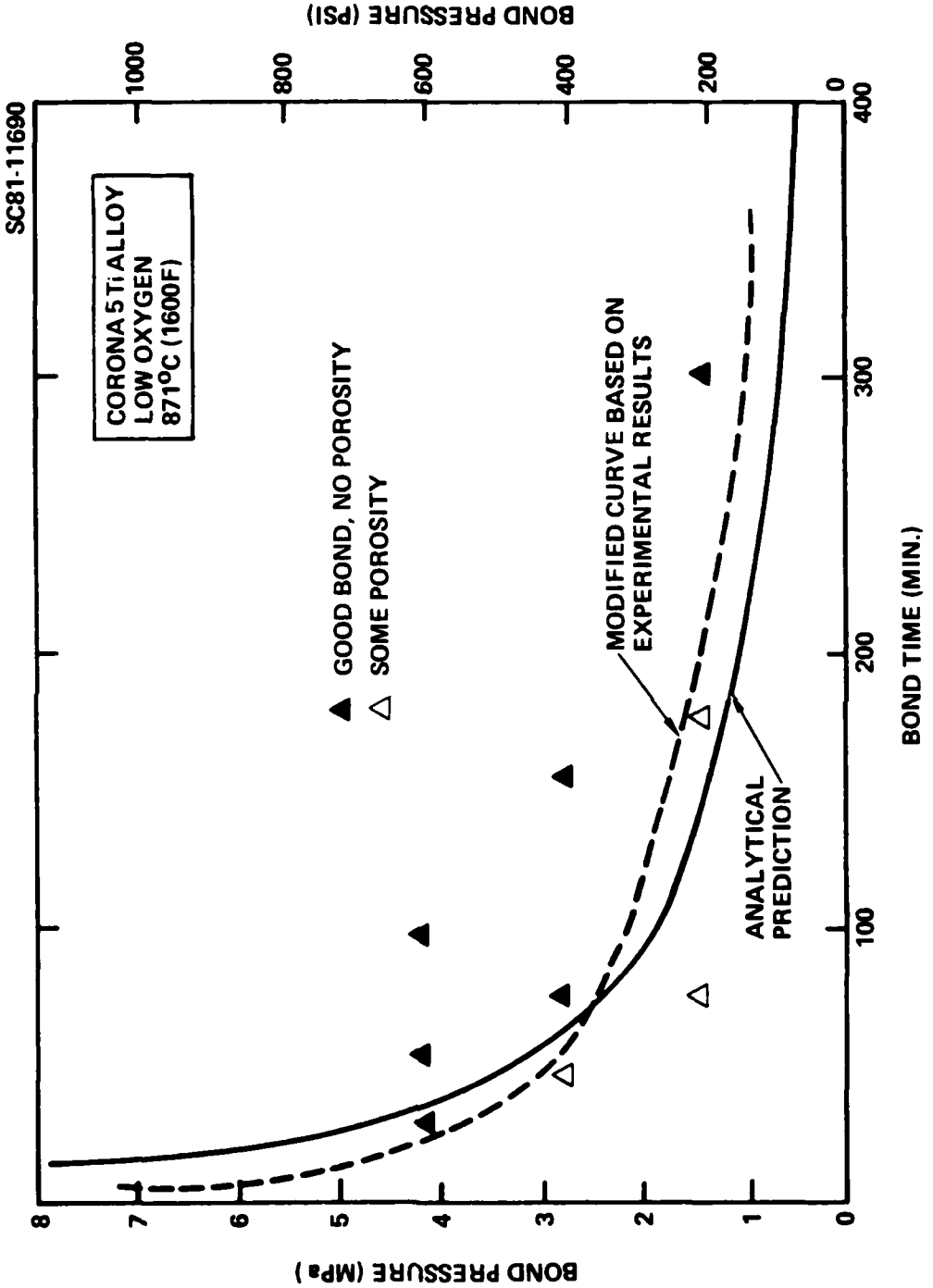

Fig. 20 Comparison of predicted bonding parameters and experimental results.

SC81-11694

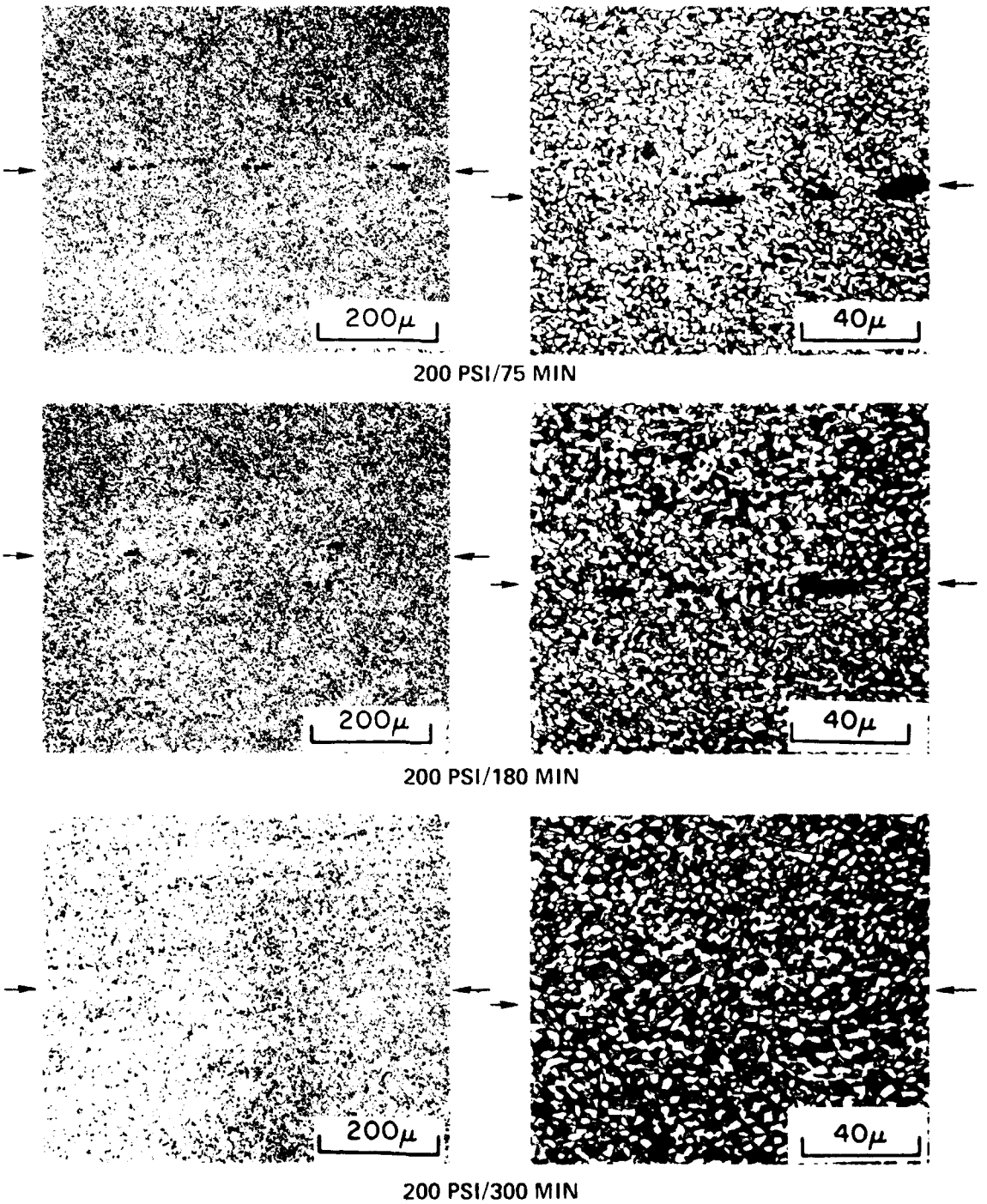

Fig. 21 Diffusion bond interfaces as a function of time for low oxygen CORONA 5 bonded at 200 psi (1.38 MPa). (100 and 500X)

SC81-11693

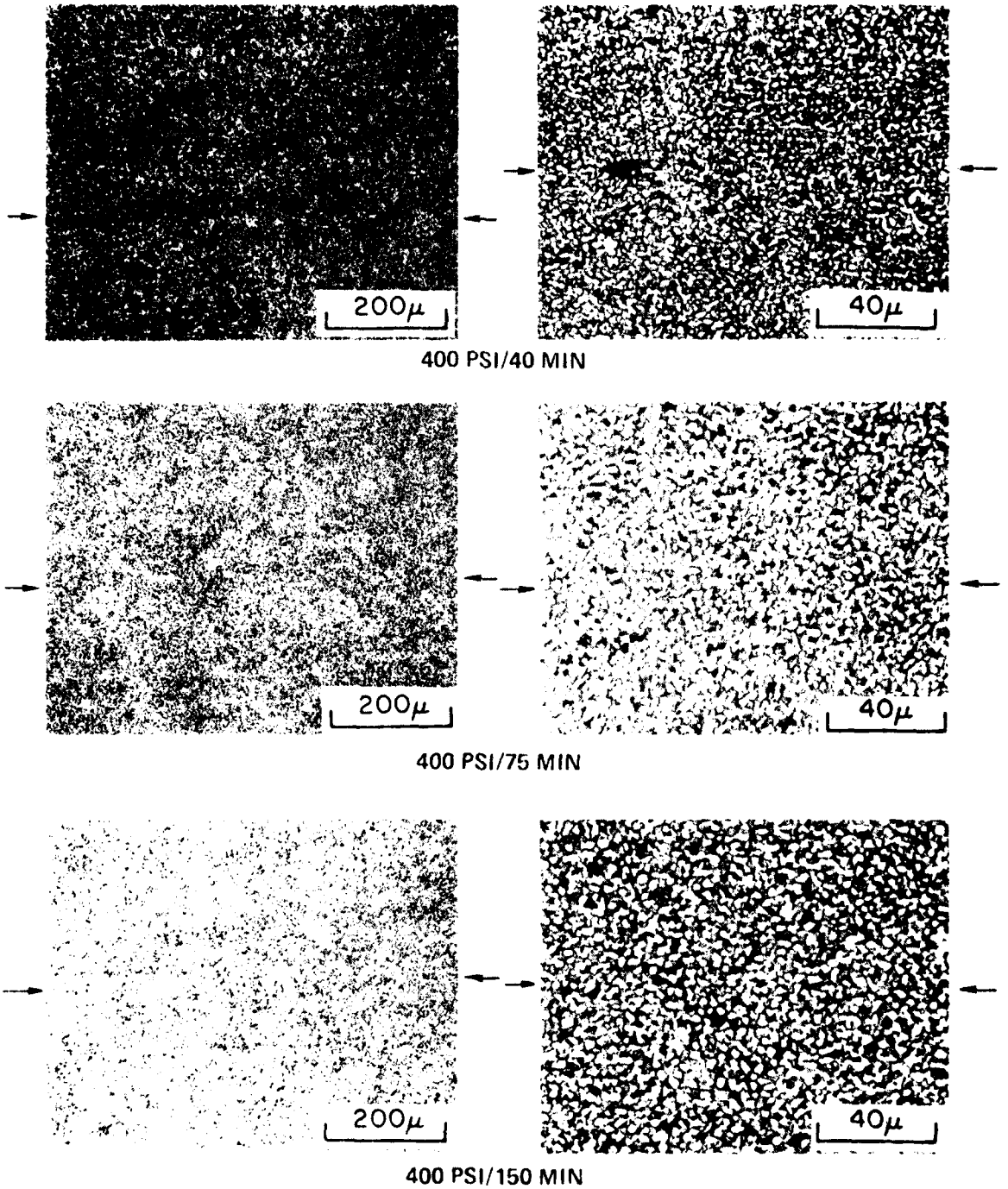

Fig. 22 Diffusion bond interfaces as a function of time for low oxygen CORONA 5 bonded at 400 psi (2.76 MPa). (100 and 500X)

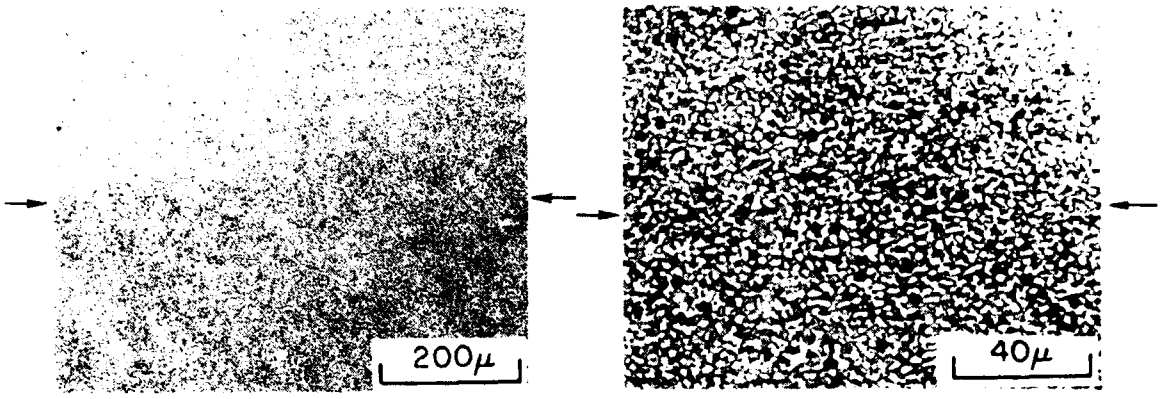

600 PSI/25 MIN

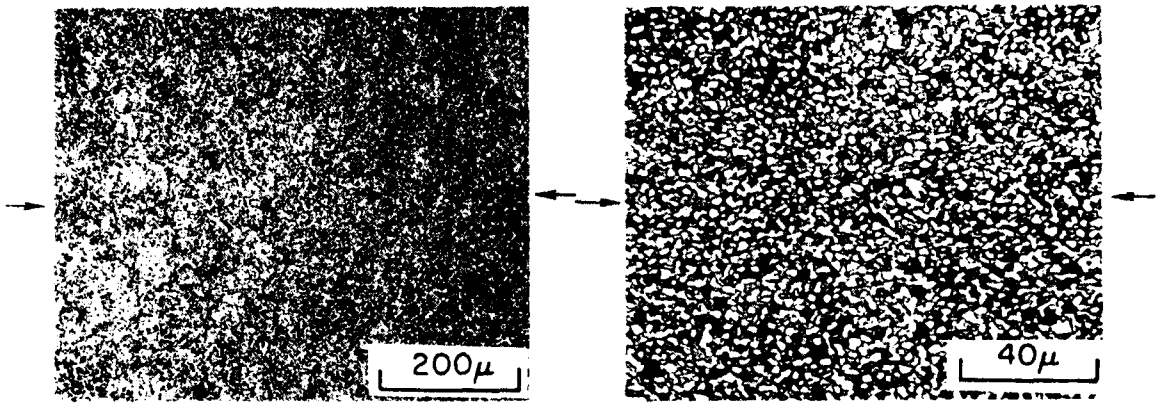

600 PSI/50 MIN

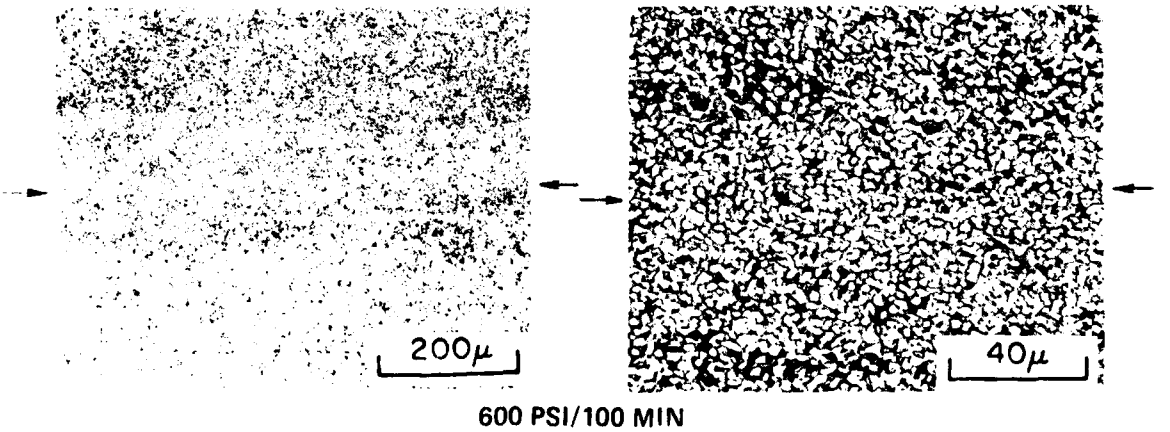

600 PSI/100 MIN

Fig. 23 Diffusion bond interfaces as a function of time for low oxygen CORONA 5 bonded at 600 psi (4.14 MPa). (100 and 500X)

bond interface can be seen in Fig. 21 for the bonding times of 75 min and 180 min. In all cases, the diffusion bond interface was virtually indistinguishable from the surrounding parent metal in areas where there was an absence of voids . This indicates there is no contamination or other deterent to achieving complete bonding other than lack of adequate metal flow at the interface. Thus, CORONA 5 is diffusion bondable and should provide bond qualities comparable to those of Ti-6Al-4V.

3.5 SPF/DB Sandwich Fabrication

In the sandwich fabrication study, the results of the superplastic forming and diffusion bonding studies were combined, and a panel fabricated using standard SPF/DB techniques. The parameters used for sandwich fabrication were based on the "best" parameters identified in the tensile, forming, and diffusion bonding studies discussed previously. The sandwich panel, shown in Fig. 24, was formed without complication. The core in this sandwich panel was well formed into the truss core configuration as can be seen in Fig. 25, where one end of the SPF/DB sandwich panel has been removed to reveal the interior of the sandwich. The core and sandwich configuration as shown in Fig. 26 also illustrates an end view of the panel corresponding to the section shown in Fig. 25.

The diffusion bonds of the panel were examined metallographically as shown in Fig. 27. The diffusion bond appears to be of good quality, although there were some areas where some microporosity was present. The source of this microporosity may be related to entrapment of argon gas used during the

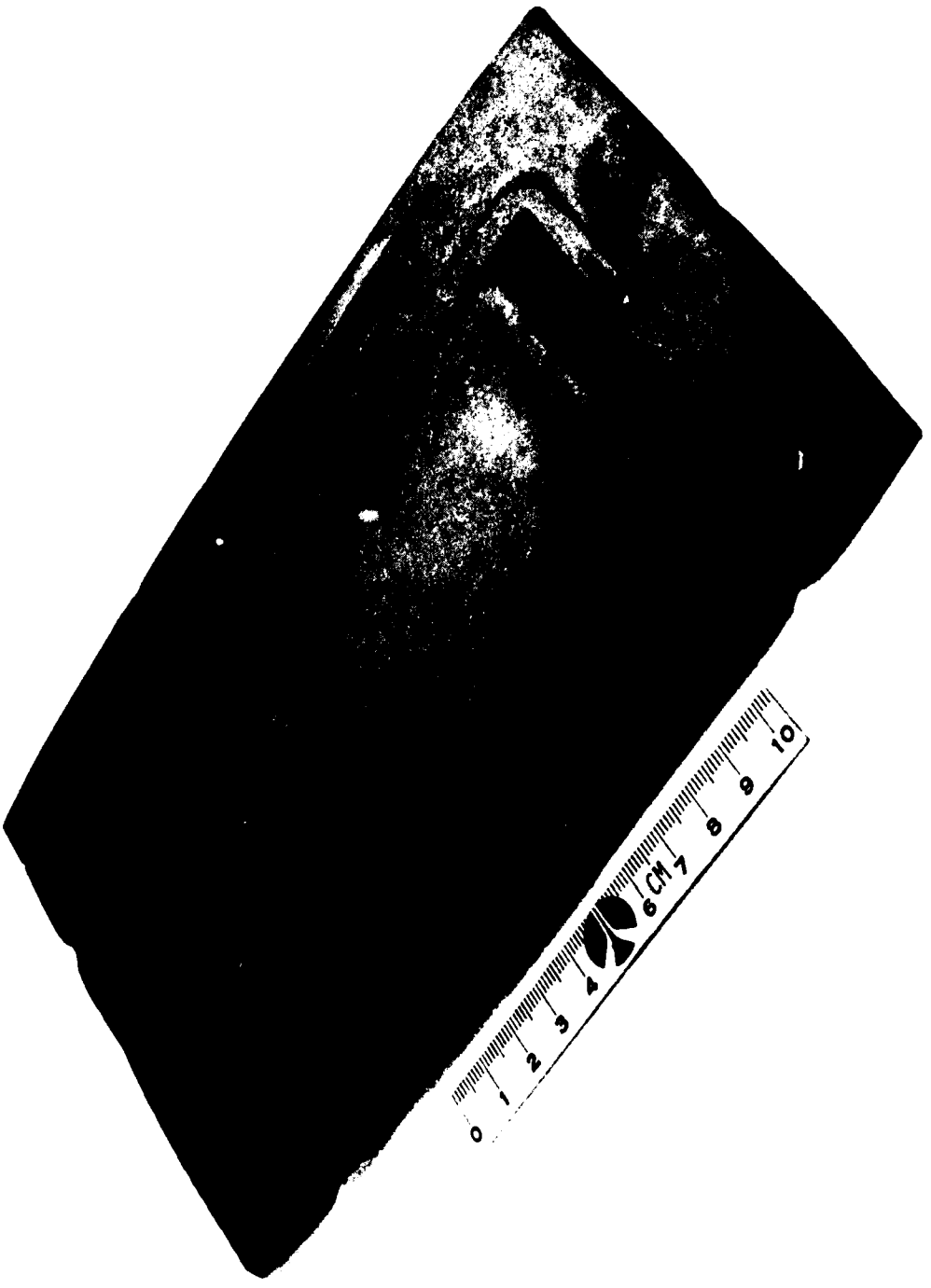

Fig. 24 CORONA 5 expanded sandwich part.

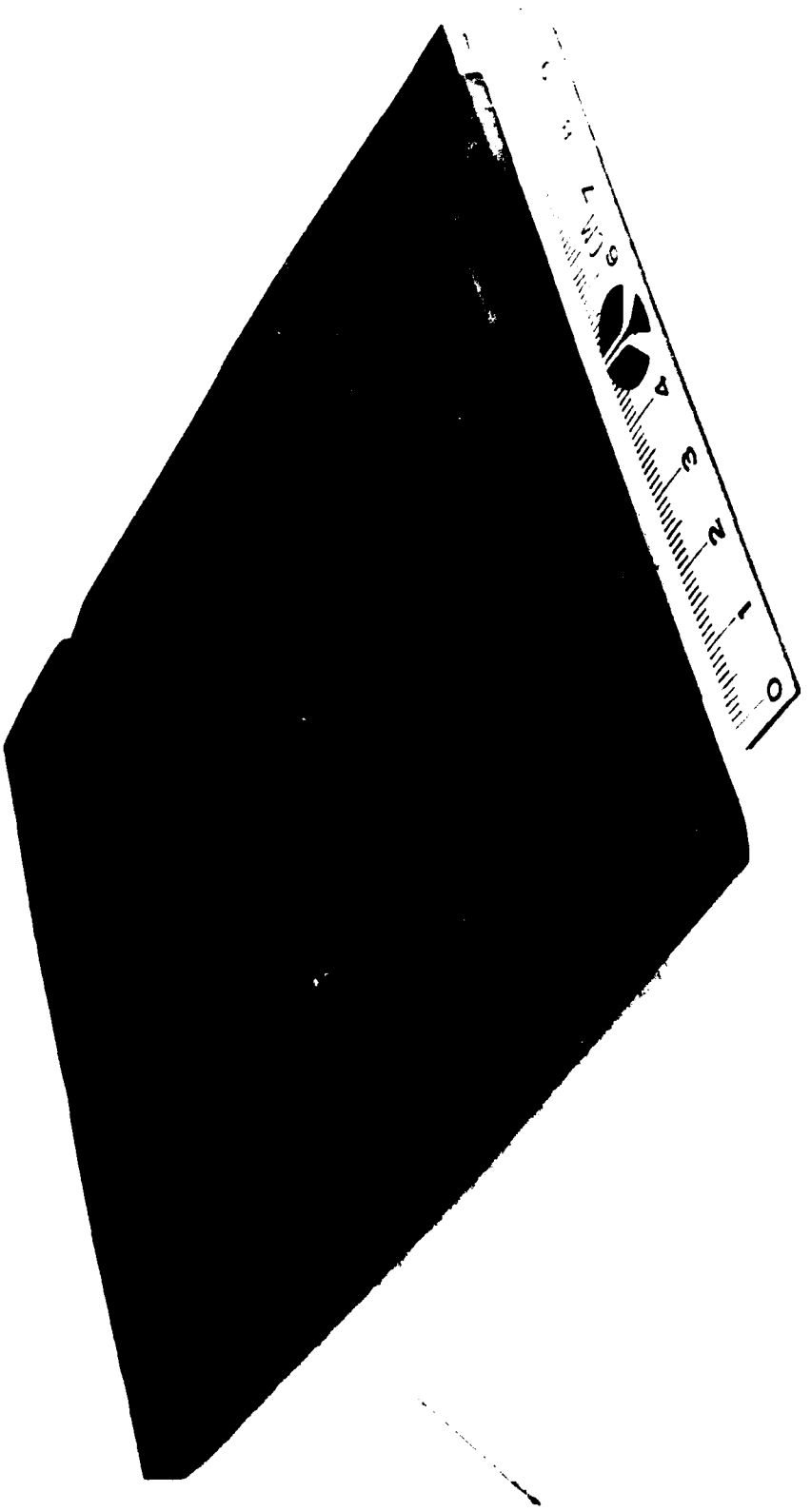

Fig. 25 Section of expanded sandwich showing truss core configuration.

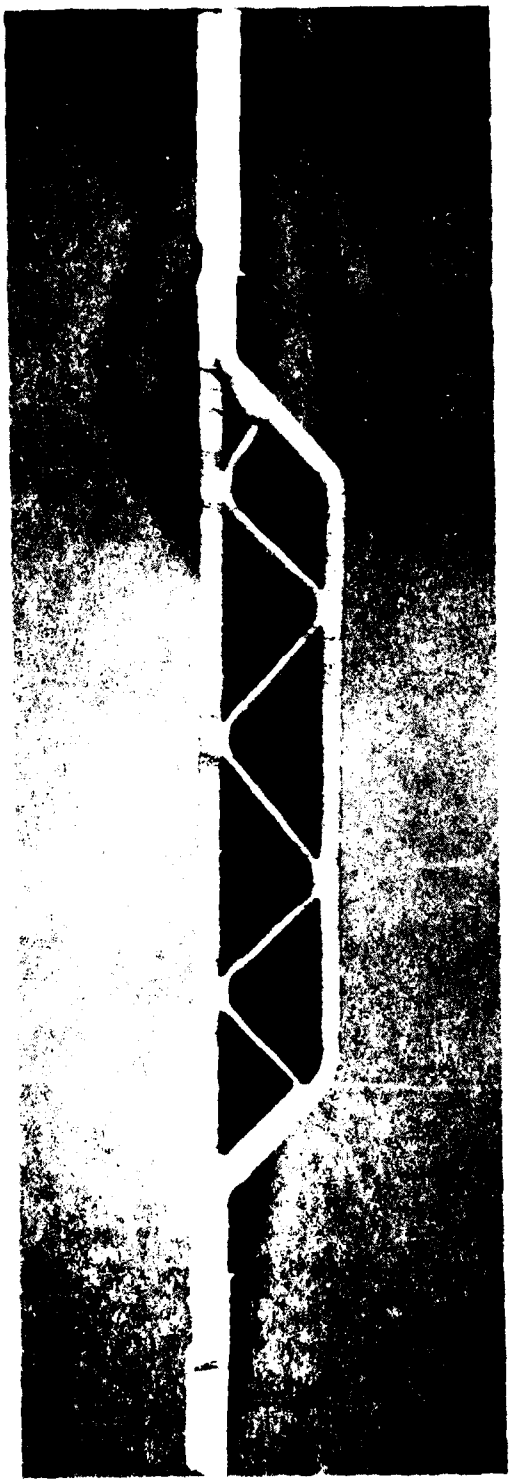

Fig. 26 End view of truss core sandwich part.

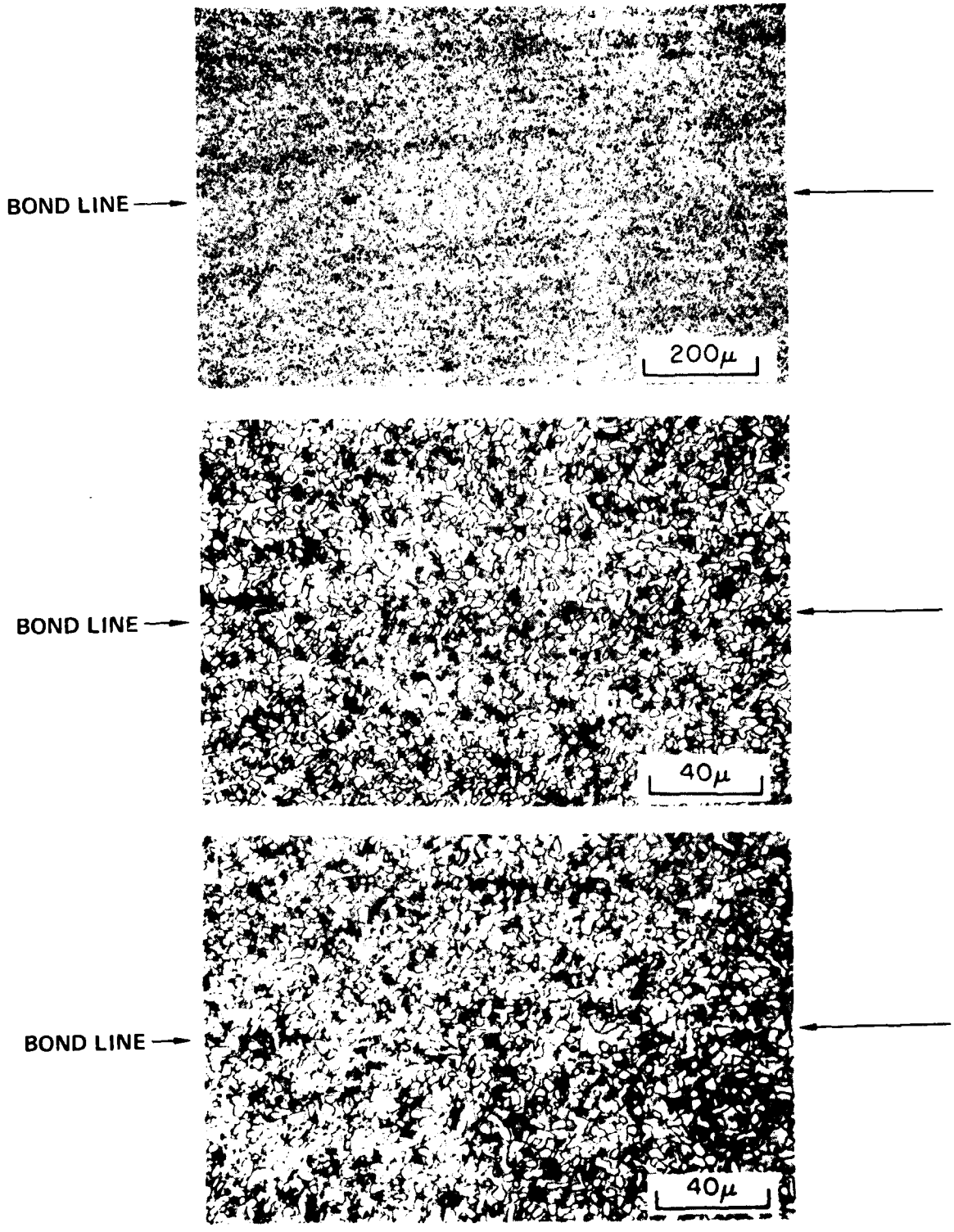

Fig. 27 Diffusion bond area from truss core sandwich. (100 and 500X)

SPF/DB processing, or it may be the result of a slight temperature drop during processing that correspondingly raises the required bonding pressure or time to achieve full bonding. The minor amount of microporosity observed in this diffusion bond is not considered to be a significant problem in the SPF/DB processing of the CORONA 5 since a minor change in the bond time and or bond pressure would be adequate to eliminate such microporosity. For manufacturing of CORONA 5 SPF/DB parts, it would be advisable to utilize a somewhat higher pressure or longer time to compensate for such variations.

Through the series of tests conducted on the CORONA 5 it has been shown that this alloy, when properly processed to fine grain sheet, does exhibit significant degree of superplasticity at elevated temperatures. The material can also be diffusion bonded and can be SPF/DB processed to produce a range of configuration such as the sandwich panel shown in Fig. 24. From the data generated, it is apparent that the optimum temperature for superplasticity in the CORONA 5 alloy is about 871°C although there is indication of substantial latitude in permissible processing temperatures. At temperatures above about 871°C, decreasing superplasticity and increased bonding pressures requirements may be necessary. It appears that the low oxygen content alloy is superior to the standard oxygen content from the standpoint of superplasticity and bond pressure requirements. However, the standard oxygen content alloy appears to be adequately superplastic and diffusion bondable and exhibits no critical deterrents in SPF/DB processing.

The indications that temperatures above 871°C result in decreased superplasticity and increased bond pressures for diffusion bonding are may be

related to a combination of factors including (1) increased grain growth kinetics, and (2) proximity to β-transus temperature. The latter may also relate to grain coarsening since it has been observed in other alloys that grain coarsening increases rapidly as the β-transus temperature is approached. The ratio of α and β phases should be approximately one for optimum superplastic properties, and temperatures at which the larger volume fraction is β phase may be less desirable for forming.

In summary, CORONA 5 Ti alloy can be processed by superplastic forming and diffusion bonding at temperatures in the range of 843 to 871°C. These are temperatures somewhat lower than those normally utilized for the Ti-6Al-4V alloy (approximately 900 - 920°C). While this alloy can be processed at lower temperatures and appears to be very promising for the SPF/DB applications it should be recognized also that the Ti-6Al-4V titanium alloy exhibits comparable superplastic properties at these lower temperatures. Combined with the heat treatment response discussed in the following section, the SPF/DB characteristics of CORONA-5 make the alloy an attractive candidate for SPF/DB parts.

3.6 Post Forming Tensile Tests

The tensile tests conducted on superplastically formed material are summarized in Table 6. Included in the table are data for standard oxygen material (R52071) which had not been formed but was tested in several conditions. A summary of the strain accumulated in the specimens during superplastic deformation of the pans from which the specimens were cut is also

included in the table. The designations e_L and e_T represent respectively, strain in the sheet parallel to and perpendicular to the long axis of the pan. The orientation for e_L corresponds to the rolling direction of the sheet and the tensile axis of specimens removed from the pans.

The tensile specimens from pans formed of low oxygen material (V5834) exhibited strange behavior. The as-formed material had yield strengths that were considerably less than their ultimate tensile strengths. The specimens removed from the pan that experienced the greatest deformation (Part No. 4, e_T = 100-140%) had the lowest yield strength (probably as a result of low initial dislocation density and increased barrier spacing associated with larger strains and longer forming times). When material from the low oxygen pans was solution treated and aged, the yield strengths of both pans (No. 1 and No. 4) were comparable. The maximum strength levels obtainable by heat treating the low oxygen material using only air-cooling is in the range of 825-860 MPa (120-125 ksi) for yield strength and 930-965 MPa (135-140 ksi) for ultimate strength.

In contrast, the standard oxygen material exhibited a potential for a strong heat treatment response as evidenced by the 1105 MPa (160 ksi) yield strength and 1170 MPa (170 ksi) ultimate tensile strength of the sheet exposed to the simulated DB and age cycle. The ability to achieve high strength levels was further demonstrated by the specimens cut from an as-formed pan which had yield and ultimate strengths of 1033 MPa (150 ksi) and 1134 MPa (165 ksi) respectively. The greatest strength levels in the high oxygen material were obtained with some loss of ductility. The ductility could be improved by

a slight reduction of oxygen levels, or by optimization of heat treatments. These are potential areas for future research and were not part of the present program.

4.0 CONCLUSIONS

1. The CORONA 5 alloy is more amenable to coil sheet processing than Ti-6Al-4V. CORONA 5 can be cold rolled up to 48% in the laboratory without edge cracking. A relatively low temperature short time strand line anneal can be used between cold rolling cycles.

2. CORONA 5 has good room temperature formability as measured by bend and Olsen Cup tests.

3. The alloy can be SPF/DB processed using the same techniques as are used for Ti-6Al-4V. The optimum temperature range for SPF/DB processing of this alloy is 843 to 871°C (1550 to 1600°F).

4. The alloy exhibited the potential for post forming heat treatment to the 1035-1135 MPa (150-165 ksi) ultimate strength level.

5.0 ACKNOWLEDGEMENTS

The authors would like to acknowledge the experimental assistant of M. Calabrese, J.M. Curnow, A.R. Murphy and L.F. Nevarez of the Science Center and C.E. Rader and S.L. Vogel of Crucible Research Center. Helpful discussions with Dr. A.K. Ghosh of the Science Center and Dr. F.H. Froes of the Air Force Wright Aeronautical Laboratory also contributed to the success of the program.

6.0 REFERENCES

1. F.H. Froes, J.C. Chesnutt, C.F. Yolton, C.H. Hamilton and M.E. Rosenblum: Proceedings of the Fourth International Titanium Conference, May (1980).

2. G.R. Keller, J.C. Chesnutt, F.H. Froes and C.G. Rhodes, Final Report, Naval Air Systems Command Contract N00019-76-C-0427, "Fracture Toughness in Titanium Alloys," NA-78-917, December (1978).

3. A.K. Ghosh and C.H. Hamilton, "Mechanical Behavior and Hardening Characteristics of a Superplastic Ti-6Al-4V Alloy," Met. Trans. 10A, p. 699, June 1979.

4. A.K. Ghosh and C.H. Hamilton, "Superplastic Forming of a Long Rectangular Box Section - Analysis and Experiment," Proceedings, Fall ASM Materials Congress, Chicago, 1979.

5. C.H. Hamilton, et al., "Superplastic Forming of Titanium Structures," AFML-TR-75-62, April 1975.

6. C.H. Hamilton, "Pressure Requirements for Diffusion Bonding Titanium," Proceedings, 2nd International Conference on Titanium, May 1974.

7. G. Garmong, N.E. Paton and A.S. Argon, "Attainment of Full Interface Contract During Diffusion Bonding," Met. Trans. 6A, p. 1269, June 1975.

8. E.D. Weisert, G.W. Stacher and B.W. Kim, "Manufacturing Methods for Superplastic Forming/Diffusion Bonding Process," AFML-TR-79-4053, May 1979.

9. J.C. Chesnutt, "Influence of Microstructure and Interstitial Elements on Fatigue Crack Propagation of CORONA 5 Titanium Alloys," Contract No. N00019-79-C-0540, Naval Air Systems Command, 1979.

Table 1

Standard Oxygen CORONA 5 Starting Material

Supplier:	Crucible							
Heat No.:	R52071							
Section/Size:	2 pieces 5 in. (127 mm) wide × 3 in. (76 mm) thick × 3-1/2 in. (89 mm) long							
Chemistry:	Weight Percent							
	Al	Mo	Cr	Fe	C	N	O	Ti
	4.4	5.1	1.46	0.20	0.065	0.011	0.183	Bal.
Condition:	As Hot Rolled							

Table 2

Low Oxygen CORONA 5 Starting Material

Supplier:	TIMET						
Heat No.:	V5834						
Section/Size:	1 piece 6 in. (152 mm) wide × 1 in. (25 mm) thick × 22 in. (559 mm) long						
Chemistry:	Weight Percent						
	Al	Mo	Cr	Fe	N	O	Ti
	4.77	5.00	1.55	0.07	0.004	0.085	Bal.
Condition:	As Hot Rolled						

Table 3

SPF Forming Study Schedule

Part No.	Heat	Temperature	Strain Rate	Configuration
1	V5834 (Low Oxygen)	871°C (1600°F)	2×10^{-4} s^{-1}	Rectangular Pan
2	V5834	871°C (1600°F)	6×10^{-4} s^{-1}	Rectangular Pan
3	V5834	871°C (1600°F)	10^{-3} s^{-1}	Rectangular Pan
4	V5834	871°C (1600°F)	2×10^{-4} s^{-1}	Deep Rectangular Pan
5	V5834	899°C (1650°F)	2×10^{-4} s^{-1}	Rectangular Pan
6	V5834	843°C (1550°F)	6×10^{-4} s^{-1}	Rectangular Pan
7	V5834	843°C (1550°F)	10^{-3} s^{-1}	Rectangular Pan
8	V5834	871°C (1600°F)	2×10^{-4} s^{-1}	Cylindrical Part
9	V5834	871°C (1600°F)	10^{-3} s^{-1}	Cylindrical Part
10	R52071 (Standard Oxygen)	871°C (1600°F)	2×10^{-4} s^{-1}	Rectangular Pan
11	R52071	871°C (1600°F)	10^{-3} s^{-1}	Rectangular Pan

Table 4

Room Temperature Properties of Simulated CORONA 5 Coil Sheet
[0.070 in. (1.8 mm) thick]

Heat No.	Heat Treatment	Test Direction	Tensile Strength (ksi)	Yield Strength 0.2% Offset (ksi)	Elongation in 2 in. (%)	Reduction of Area (%)	E x10^6 psi	Bend† R/t	Olsen Cup Height (in.)	Olsen Cup O_2 (%)	Olsen Cup H_2 (%)
R52071	1400°F/5min/AC	long	148.2	142.2	7.5	30.1	15.5	3.2	0.140	0.168	0.0055
		long	149.7	144.0	4.5	31.0	14.9		0.150	0.170	0.0058
		trans	166.9	166.6	4.0	33.2	17.8	4.7			
		trans	180.4	179.8	4.0	26.2	18.6				
V5834	1400°F/5min/AC	long	145.2	134.4	10.5	49.3	15.1	2.4	0.26	0.069	0.0062
		long	143.1	130.6	11.5	46.4	13.8		0.220	0.070	0.0062
		trans	157.7	-	<1.0*	48.2	15.0	3.5			
		trans	160.7	159.8	1.0*	46.2	16.6				
Specification Mil-T-9046											
STD Ti-6Al-4V			134 min	126 min	10 min			4.5 max 0.12 (Typical)			
ELI Ti-6Al-4V			130 min	120 min	10 min			4.5 max			

†R = Die Radius, t = Material Thickness
Values represent minimum radius without cracking.
*Fracture occurred outside gage marks.
1400°F = 760°C
1 ksi = 6.894757 MPa

Table 5

Summary of Tensile Elongation Test Data

Heat	Temp (°F)	$\dot{\varepsilon}$ (s^{-1})	Elong.(%)	m*
R-52071	1550	1×10^{-4}	420	0.90
(Standard	1550	2×10^{-4}	480	0.72
Oxygen)	1550	1×10^{-3}	190	0.36
	1550	5×10^{-3}	>195	0.42
	1600	2×10^{-4}	>510	0.63
	1600	11×0^{-3}	320	0.55
	1600	5×20^{-3}	205	0.52
	1600	1×10^{-2}	100	0.50
	1650	2×10^{-4}	340	0.68
	1650	1×10^{-3}	>370	0.56
	1650	5×10^{-3}	180	0.48
	1650	1×10^{-2}	120	0.45
V-5834	1550	2×10^{-4}	500	0.74
(Low	1550	1×10^{-3}	320	0.62
Oxygen)	1550	5×10^{-3}	380	0.57
	1550	1×10^{-2}	280	0.58
	1600	2×10^{-4}	>380	0.81
	1600	1×10^{-3}	>340	0.65
	1600	5×10^{-3}	-	0.63
	1600	1×10^{-2}	260	0.70
	1650	2×10^{-4}	300	0.64
	1650	1×10^{-3}	300	0.57
	1650	5×10^{-3}	160	0.46
	1650	1×10^{-2}	140	0.42

*From step/strain rate tests.
1550°F = 843°C
1600°F = 871°C
1650°F = 899°C

Table 6
Post-Forming Tensile Results

Heat No.	Spec No.	Condition	$\sigma_{0.2}$ ksi	$\sigma_{0.2}$ MPa	σ_u ksi	σ_u MPa	e (%)	RA (%)	Forming Temp °F	Forming Temp °C	Forming Time min	Superplastic Strain e_L (%)	Superplastic Strain e_T (%)	Part No.[1]	Spec No.
V5834	305-1	As-formed	122	841	162	1114	28	6	1600	871	102	5	35	1	305-1
V5834	305-2	As-formed + STA[2]	121	834	137	946	9	7	1600	871	102	5	35	1	305-2
V5834	308-1	As-formed	78	538	132	910	13	10	1600	871	180	5	140	4	308-1
V5834	308-2	As-formed + STA[2]	124	855	138	951	8	10	1600	871	180	0	100	4	308-2
R52071	-	CR + A[3]	149	1024	154	1058	14	20							
R52071	-	CR + A + Sim DB[4]	150	1034	166	1062	10	17							
R52071	-	CR + A Sim DB + A[5]	160	1100	170	1169	8	8							
R52071	301-1	As-formed + STA[6]	128	880	146	1009	6	7	1600	871	20	10	50	11	301-1
R52071	301-2	As-formed + STA[6]	137	942	150	1033	5	7	1600	871	20	10	30	11	301-2
R52071	306-2	As-formed + STA[6]	150	1033	165	1134	4	13	1600	871	142	14	52	10	306-2

Notes:
(1) See Table 3
(2) 1525°F (829°C)/4 hr/AC + 1000°F (538°C)/16 hr/AC
(3) Cold-rolled and annealed (see Section 2.1.2
(4) 1600°F (871°C)/2 hr/AC
(5) 1050°F (566°C)/8 hr/AC
(6) 1550°F (843°C)/4 hr/AC + 1000°F (538°C)/16 hr/AC


DAT
FILM